
1 **Arabidopsis AGAMOUS-LIKE16 and SUPPRESSOR OF**
2 **CONSTANS1 regulate genome-wide expression and**
3 **flowering time**

4 Xue Dong ^{1,2}, Li-Ping Zhang ¹, Yin-Hua Tang ^{1,3}, Dongmei Yu ¹, Fang Cheng ¹, Yin-Xin
5 Dong ¹, Xiao-Dong Jiang ¹, Fu-Ming Qian ¹, Zhen-Hua Guo ^{2,*}, Jin-Yong Hu ^{1,*}

6 1. CAS Key Laboratory for Plant Diversity and Biogeography of East Asia, Kunming
7 Institute of Botany, Chinese Academy of Sciences. Kunming 650201, Yunnan Province,
8 China.

9 2. Germplasm Bank of Wild Species, Kunming Institute of Botany, Chinese Academy of
10 Sciences, Kunming, Yunnan 650201, China

11 3. Kunming College of Life Sciences, University of Chinese Academy of Sciences,
12 Kunming 650201, Yunnan Province, China.

13 * **Corresponding authors:** Jin-Yong Hu (hujinyong@mail.kib.ac.cn); Zhen-Hua Guo
14 (guozhenhua@mail.kib.ac.cn)

15 **Short title:** AGL16-SOC1 collaborate to time flowering

16 The author responsible for distribution of materials integral to the findings presented in
17 this article in accordance with the policy described in the Instructions for Authors
18 (<https://academic.oup.com/plphys/pages/general-instructions>) is Jin-Yong Hu
19 (hujinyong@mail.kib.ac.cn).

20

21

22

23

24 **Author contributions**

25 J-Y H and X D conceptualized and coordinated the research; L-P Z performed the ChIP
26 and transient expression experiments and collected the RNA samples with help from X-D
27 J; Y-H T, J-Y H, and D-M Y carried out the protein interaction assays; X D, J-Y H and L-P Z
28 created the genetic materials and did the genetic analyses; X D analyzed and visualized
29 all the data; Y-H T, F C, Y-X D, X-D J, and F-M Q did the other analyses; J-Y H and X D
30 wrote the paper with help from the other authors. All authors read and approved the
31 manuscript.

32

33 **Abstract**

34 Flowering transition is tightly coordinated by complex gene regulatory
35 networks, in which AGAMOUS-LIKE 16 (AGL16) plays important roles. Here,
36 we identified the molecular function and binding properties of AGL16 and
37 demonstrated its partial dependency on SUPPRESSOR OF CONSTANS 1
38 (SOC1) function in regulating flowering. AGL16 bound to promoters of more
39 than 2000 genes via CArG-box motifs with high similarity to that of SOC1 in
40 *Arabidopsis* (*Arabidopsis thaliana*). Approximately seventy flowering genes
41 involved in multiple pathways were potential targets of AGL16. AGL16 formed
42 a protein complex with SOC1 and shared a common set of targets. Intriguingly,
43 only a limited number of genes were differentially expressed in the *agl16-1*
44 loss-of-function mutant. However, in the *soc1-2* knockout background, AGL16
45 repressed and activated the expression of 375 and 182 genes, respectively,
46 with more than a quarter bound by AGL16. Corroborating these findings,
47 AGL16 repressed the flowering time more strongly in *soc1-2* than in the Col-0
48 background. These data identify a partial inter-dependency between AGL16
49 and SOC1 in regulating genome-wide gene expression and flowering time,
50 while AGL16 provides a feedback regulation on *SOC1* expression. Our study
51 sheds light on the complex background dependency of AGL16 in flowering
52 regulation, thus providing additional insights into the molecular coordination of
53 development and environmental adaptation.

54

55 Introduction

56 Timely transitions from vegetative to reproductive growth (floral transition) and
57 from dormant to germinating seeds determine the capacity of plant adaptation
58 to changing environments, thus are under tight control by complex interactions
59 between endogenous signals and exogenous environmental factors (Michaels,
60 2009; Andres and Coupland, 2012; Nee et al., 2017). The
61 gene-regulatory-network (GRN) controlling floral transition converges at
62 several floral integrator genes like *SUPPRESSOR OF CONSTANS1* (*SOC1*)
63 and *FLOWERING LOCUS T* (*FT*). These genes often encode transcription
64 regulators controlling the transcription of their downstream targets by binding
65 to specific *cis*-motifs, for example CArG-boxes (Michaels, 2009; Fornara et al.,
66 2010; Andres and Coupland, 2012). CArG-box motifs are binding sites specific
67 for MADS-box transcription factors (TFs) like *SOC1*, *FLOWERING LOCUS C*
68 (*FLC*), *SHORT VEGETATIVE PHASE* (*SVP*) and *SEPALLATA 3* (*SEP3*)
69 (Immink et al., 2009; Kaufmann et al., 2009; Kaufmann et al., 2010; Deng et al.,
70 2011; Immink et al., 2012; Tao et al., 2012; Gregis et al., 2013; Mateos et al.,
71 2015; Mateos et al., 2017; Aerts et al., 2018). These MADS-box TFs often form
72 homo- and/or hetero- protein complexes that act in concert and bind to the
73 CArG-box motifs in promoters of more than hundreds of downstream genes to
74 regulate flowering time and other developmental processes in *Arabidopsis*
75 (*Arabidopsis thaliana*).

76 *SOC1* is one key flowering promoter integrating signals from photoperiod,
77 temperature, hormones and age-related pathways (Lee and Lee, 2010). *SOC1*
78 forms protein complex with *AGL24* to activate *LFY* and *AP1* to initiate and
79 maintain flower meristem identity but represses *SEP3* to prevent premature
80 differentiation of floral meristem (Lee et al., 2008). *SOC1* activates the
81 expression of *TARGET OF FLC AND SVP1* (*TFS1*) via recruiting histone
82 demethylase *RELATED TO EARLY FLOWERING 6* (*REF6*) and chromatin
83 remodeler *BRAHMA* (*BRM*), and cooperates with *SQUAMOSAL PROMOTER*
84 *BINDING PROTEIN-LIKE 15* (*SPL15*) to modulate their targets expression
85 thereby regulating flowering time (Hyun et al., 2016; Richter et al., 2019).

86 SOC1 forms a set of heterologous complexes with other MADS-box TFs (de
87 Folter et al., 2005; Immink et al., 2009). Furthermore, *SOC1* times flowering
88 downstream of several hormone signaling pathways including GA, ABA and
89 BRs (Jung et al., 2012; Li et al., 2017; Hwang et al., 2019) and of nutrient
90 status (Liu et al., 2013; Olas et al., 2019; Yan et al., 2021). Interestingly,
91 profiling of *SOC1* targets also identifies genes involved in the signaling
92 processes of these hormones and nutrients (Immink et al., 2012; Tao et al.,
93 2012). Via protein complexing with many TFs and binding to its own promoter,
94 *SOC1* regulates its own expression with auto-regulatory feedback loops
95 (Immink et al., 2012). However, the biological importance of these molecular
96 interactions remains to be explored further.

97 *AGL16* is a floral repressor with dependency on genetic background,
98 photoperiod of growth conditions, and gene dosages (Hu et al., 2014). Only
99 under the inductive long-day conditions loss-of-function mutants for *AGL16*
100 show early flowering especially in the functional *FRI-FLC* background
101 (Johanson et al., 2000; Michaels and Amasino, 2001; Hu et al., 2014). *AGL16*
102 expression can be modulated by the level of the Brassicaceae-specific *miR824*,
103 for which natural variation has been identified (Rajagopalan et al., 2006;
104 Fahlgren et al., 2007; Kutter et al., 2007; de Meaux et al., 2008; Hu et al.,
105 2014). Change in *miR824* expression results in a significant modification of the
106 plant flowering (Hu et al., 2014). *AGL16* acts in flowering time regulation via
107 transcriptional regulation of *FT*, whose expression is also regulated by TFs like
108 SVP and FLC and many others (Aukerman and Sakai, 2003; Searle et al.,
109 2006; Jung et al., 2007; Castillejo and Pelaz, 2008; Li et al., 2008; Mathieu et
110 al., 2009). *AGL16* forms complexes with SVP and FLC, and mildly represses
111 their expression (Hu et al., 2014). *AGL16* is a direct downstream target of both
112 FLC and SVP, but the expression of *AGL16* changes only weakly in
113 loss-of-function mutants of both genes (Deng et al., 2011; Gregis et al., 2013;
114 Mateos et al., 2015). Yeast-two-hybrids assays suggest that *AGL16* interacts
115 with *SOC1* and other MADS-box TFs and is hypothesized to modulate the
116 *SOC1* expression (de Folter et al., 2005; Immink et al., 2009; Immink et al.,
117 2012). Besides its roles in development (Kutter et al., 2007; Hu et al., 2014),
118 *AGL16* represses plant responses to salt stress and drought resistance via

119 binding to a specific set of downstream genes (Zhao et al., 2020; Zhao et al.,
120 2021). The *miR824-AGL16* module participates also in heat stress adaptation
121 (Szaker et al., 2019). However, the exact AGL16 target spectra and the
122 impacts of interactions between AGL16 and its partners remain
123 under-explored.

124 In this study, we profiled the target spectra of AGL16 and demonstrated the
125 molecular and genetic links between AGL16 and SOC1 played important roles
126 in flowering time regulation. We found that, in contrast to its weak effects in
127 flowering time regulation in Col-0 background, AGL16 could bind to more than
128 2000 target genes that were involved in regulation of flowering time and many
129 other biological processes. We showed that the regulatory roles of AGL16 on
130 genome-wide gene expression and flowering time depended partially on the
131 SOC1 activity.

132 **Results**

133 **AGL16 binds to a large set of genomic segments with CA_nG boxes**

134 We profiled AGL16 binding sites by a ChIP-seq approach (chromatin
135 immuno-precipitation followed by sequencing). We used a line expressing
136 *AGL16* fused to a combined Yellow Fluorescent Protein (YFP) -HA epitope tag
137 under the control of the Cauliflower Mosaic Virus 35S promoter (*AGL16OX*),
138 which restores the early flowering of *agl16-1* to wild type Col-0 level (Fig. S1)
139 (Hu et al., 2014). In two independent trials, we identified respectively 5463 and
140 3294 DNA segments statistically enriched for AGL16 binding, of which 3086
141 were shared (Table S1, S2). Most of the peaks were around 150-500 bp in
142 both trials (Fig. S2). To test whether these segments were real binding sites for
143 AGL16, we carried out ChIP-qPCR assays with two independent chromatin
144 preparations for 20 peaks identified by ChIP-seq. These efforts confirmed 12
145 regions bound by AGL16-YFP-HA with a minimum two-fold enrichment in the
146 *AGL16OX* line compared to *agl16-1* background (Fig. 1). Besides these, four
147 known targets including *HKT1;1* (AT4G10310), *HsfA6a* (AT5G43840),

148 *MYB102* (AT4G21440), and *CYP707A3* (AT5G45340) were also among the
149 list (Zhao et al., 2020; Zhao et al., 2021). Hence, a majority proportion of peaks
150 detected via ChIP-seq method were reproducibly enriched.

151 Peaks bound by AGL16 were annotated using Arabidopsis TAIR10 data to
152 identify their distribution and genomic features (Fig. 2). The peaks from both
153 trials were centered to the 3 Kb regions around transcriptional start sites (TSS;
154 Fig. 2B). Around 60% of peaks located in the 1 Kb regions surrounding TSS
155 (Fig. 2C; Table S2). About 10% of peaks were in the 1-2 kb promoter regions
156 upstream of TSS, while 10-12% of peaks were in exons/introns. Thus, AGL16
157 bound to DNA fragments close to TSS of a large set of genes. The 2339 genes
158 with peaks mapped to gene body or up to 2 Kb upstream of their TSS were
159 taken as AGL16 targets (Table S2).

160 We next searched for potential cis-motifs in the common peaks bound by
161 AGL16 using HOMER, which could predict new motifs and identify known
162 motifs (Heinz et al., 2010). This analysis reported a *de novo* CArG-box motif
163 CCATTTTTGG for AGL16 in 707 peaks (24.2% of all common peaks; Fisher
164 $P=1e-340$, in comparison to 3.8% at genome level; Fig. 2D, Table S2). Ten
165 other CArG-box motifs were also significantly enriched, and matched to the
166 known motifs of SVP, SOC1, SEP3, TAGL1, AGL63, and other MADS-box TFs,
167 most of which could potentially interact with AGL16 (Fig. 2D; Fig. S3; Table S2).
168 The *de novo* and the ten significantly enriched CArG-box motifs were all
169 distributed around the peak center, indicating that AGL16 bound to its targets
170 via the cluster of CArG-box motifs, just like SOC1 and other MADS-box
171 proteins (Deng et al., 2011; Immink et al., 2012; Tao et al., 2012). There were
172 also other motifs significantly enriched in the AGL16 bound peaks, such as
173 those bound by TCPs (321 peaks), bHLHs (1131), C2C2 DOFs (2524),
174 WRKYs (1039). However, these motifs were not in the peaks center. Since
175 AGL16 modulated significantly the flowering time in *Arabidopsis* (Hu et al.,
176 2014), we next asked which flowering time genes could be targeted by AGL16.

177 **AGL16 targets flowering time genes in multiple pathways**

178 The Arabidopsis genome contains ~400 flowering time genes, among which
179 around 70 were targeted by AGL16 (Fig. 3; Table S2). This number was
180 significantly larger than randomly expected (*Yates' Chi-square test*, $p < 0.0001$).
181 Consistent with the described photoperiod dependency for AGL16-mediated
182 flowering regulation (Hu et al., 2014), 37 genes (for example *AGAMOUS LIKE*
183 *15/16/18* (*AGL15/AGL16/AGL18*), *CONSTANS LIKE 1/3/4/5* (*COL1/3/4/5*),
184 *TWIN SISTER OF FT* (*TSF*) and *MOTHER OF FT* (*MFT*), etc.) were related to
185 photoperiod and circadian clock pathways (Bouche et al., 2016). Ten genes
186 (like *AGL19* and *SVP*, etc.) were in the vernalization and ambient temperature
187 pathway, seven genes were involved in the gibberellin acid (GA) pathway, and
188 nine genes are integrators or related to meristem response and developmental
189 process. Four genes bound by AGL16 were not clearly defined for the
190 flowering pathways (Boxall et al., 2005; Xiao et al., 2009; Zhao et al., 2011).
191 Taken together, AGL16 might impact several flowering pathways, and the
192 alteration of flowering time in mutants of *AGL16* could be a net effect of
193 multiple flowering pathways.

194 **AGL16 binds to *SOC1* promoter and modifies its expression**

195 The floral integrator gene *SOC1* was one of the targets bound by AGL16 (Fig.
196 4A; Table S2). AGL16 interacted with three DNA segments (peaks 1389, 1390
197 and 1391) in the promoter region of *SOC1* that harbored several CARG-motifs,
198 consistent with a previous observation that the whole intergenic region is
199 required for proper *SOC1* expression (Hepworth et al., 2002). Peak 1390
200 overlapped with a region bound by *SOC1* itself (*SOC1* binding region 1) (Tao
201 et al., 2012), while peak 1389 overlapped with regions previously shown to be
202 targeted by *SVP* (Tao et al., 2012; Mateos et al., 2015) or *FLC* (Deng et al.,
203 2011; Mateos et al., 2015). An independent ChIP-qPCR assay confirmed
204 AGL16 binding on all three peaks with the binding on peaks 1389 and 1391
205 relatively stronger than on peak 1390 (Fig. 4B). The second segment bound by
206 *SOC1* itself (*SOC1* binding region 2 or fragment 7) was not targeted by AGL16.
207 As AGL16 forms protein complexes with *SVP* and *FLC* (Hu et al., 2014), it is
208 likely that AGL16 binds target regions together with these MADS-box TFs.

209 However, *SOC1* transcription was weakly upregulated by loss-of-function of
210 *AGL16* in both Col-0 (Fig. 4C) and Col-*FRI* backgrounds (Fig. S4), a pattern
211 likely caused by the very complex regulation of *SOC1* expression (Hepworth et
212 al., 2002; Immink et al., 2012). A transient luciferase assay with the 1.7 Kb
213 *SOC1* promoter in *N. benthamiana* leaves demonstrated that the
214 co-transfection of *AGL16* significantly repressed the *pSOC1* expression
215 compared to the co-transfection control with an empty vector (Fig. 4D; S5). In
216 contrast, when the CArG box(es) bound by MADS-box TFs were mutated (m3,
217 m456, and m3456), *pSOC1* expression increased remarkably, and this
218 increase became even more prominent when *AGL16* was co-transfected
219 additionally. These data together suggest that *AGL16* represses directly the
220 *SOC1* expression.

221 **AGL16 forms protein complex with SOC1**

222 *AGL16* dimers likely with *SOC1* (Fig. S3) (de Folter et al., 2005; Immink et al.,
223 2009). We verified this interaction with Yeast-2-Hybrid (Y2H) and bimolecular
224 fluorescence complementation (BiFC) techniques. Y2H assays confirmed
225 interactions between *SOC1* and *AGL16* (Fig. 5A), which was as strong as the
226 previously reported direct interaction between *AGL16* and *SVP*, in clear
227 contrast to the negative interaction between *AGL16* and *LHP1* (Hu et al., 2014).
228 BiFC assays by fusing the N-terminal half of yellow fluorescent protein (nYFP)
229 with *AGL16* (35S:*AGL16-nYFP*) and the C-terminal of YFP with *SOC1*
230 (35S:*SOC1-cYFP*) detected an interaction of *AGL16* with *SOC1* in the nuclei of
231 *Agrobacterium*-infiltrated *Nicotiana benthamiana* leaves (Fig. 5B). A further
232 co-immunoprecipitation (co-IP) assay with *AGL16* fused to a YFP tag and
233 *SOC1* fused with a Flag tag in Arabidopsis cells also confirmed the physical
234 interaction between these two TFs (Fig. 5C). Hence *AGL16* and *SOC1* form
235 hetero-protein-complexes.

236 **AGL16 and SOC1 co-target a common set of genes**

237 We next examined whether *AGL16* and *SOC1* had common targets. For this

238 aim, the previously generated binding profiles for SOC1 were used to identify
239 shared targets with AGL16 (Immink et al., 2012; Tao et al., 2012). We applied
240 the same annotation procedure for both AGL16 and SOC1 binding profiles in
241 order to identify common genes. There were 193 AGL16-bound segments that
242 overlapped with 240 SOC1 peaks (Table S3). These peaks were in the +/-2 Kb
243 vicinity of 223 genes (five without annotation information), which were then
244 taken as AGL16 and SOC1 common targets (Fig. 6A). Most of these common
245 peaks were in the 1 kb region surrounding TSS with AGL16 peaks a bit more
246 proximal (Fig. 6B). We further identified 211 CARG-box motifs in 144 common
247 peaks (400 bp surrounding peak centers; 74.6% of all overlapped peaks) with
248 MEME-ChIP. Eighty-seven peaks harbored one CARG-box
249 (DCCAAAAWGGAAAR; 60.4%), while the rest featured two (49 or 34%) or
250 three (6 peaks or 4.2%) or more (2 peaks; Fig. S6A). The distances between
251 the CARG-box motifs were spaced with 20-40 bases (Fig. S6B). Among these
252 common targets, genes involved in floral organ development (or reproductive
253 growth) and responses to hormone stimulus including ethylene and ABA were
254 significantly enriched (Fig. 6C; Table S3). Eight genes of the photoperiod and
255 circadian clock related pathways (*AGL15*, *AGL18*, *ATC*, *PHYA*, *RAV2*, *SMZ*,
256 *SNZ* and *TOE3*), three genes of the temperature-related pathways (*CBF1*,
257 *CBF2* and *SVP*), and *SOC1* itself were involved in flowering (Fig. 3),
258 suggesting that AGL16 and SOC1 act likely together to time floral transition in
259 *Arabidopsis*.

260 **AGL16 regulates genome-wide gene expression depending partially on** 261 **SOC1 function**

262 We next determined to what extent the gene expression at the genome-wide
263 level could be affected by the AGL16-SOC1 module (Table S1). For this, we
264 carried out a comparative transcriptomics analysis using the single and double
265 mutants between the *agl16-1* and *soc1-2* lines. In contrast to the very broad
266 binding spectrum of AGL16, we only detected very small number of genes
267 showing differential expression (DEGs) in *agl16-1* single mutant (9 up and 12
268 down) compared to Col-0 (Fig. 7A; Table S4). The *soc1-2* single (155 up and
269 285 down) and the *agl16 soc1* double (49 up and 353 down) mutants had

270 similar number of DEGs but *soc1-2* featured more up and less down DEGs
271 (Yate's *chi-square test*, $p < 0.001$; Fig. 7A), indicating that AGL16 either
272 countered SOC1's repressive or inductive role on gene expression. A heatmap
273 analysis of DEGs in the *soc1-2* vs Col-0 revealed that absence of *agl16* mostly
274 reverted the differential gene expression observed in *soc1-2* to wild type levels
275 (Fig. 7B). Genes down-regulated in the *agl16 soc1* mutants showed also
276 down-regulation in *soc1-2* (Fig. 7C). In contrast, genes up-regulated in *agl16*
277 *soc1* were barely affected by either single mutation, suggesting that for these
278 genes, AGL16 and SOC1 contribute redundantly to the repression.
279 Accordingly, only 83 *soc1-2* DEGs (in total 155 up and 285 down; ~18.9%)
280 overlapped with the *agl16 soc1* DEGs (375 up and 182 down; ~14.9%; Fig.
281 7D). Therefore, AGL16 has potential in regulating gene expression at the
282 genome-wide level, but apparently depends on its genetic background, i.e.
283 here the SOC1 activity.

284 We next examined to what extent these DEGs associated with AGL16
285 targeting. Among the 557 *agl16 soc1* DEGs, AGL16 bound to 98 genes
286 (~22.2%), in which only 23 (~4.1%) were also targeted by SOC1 (Fig. 7D).
287 About 13.6% or 60 *soc1-2* DEGs were likely the AGL16 targets (Yate's
288 *chi-square test*, $p = 2e-8$, in comparison to genome-wide level of AGL16
289 binding). However, we noticed that only nine *soc1-2* DEGs (~2% among 440)
290 were potential targets of SOC1, a pattern similar to a previous report, in which
291 52 SOC1 targets were among the 1186 DEGs (Tao et al., 2012). There were
292 six targets (~28.6%) showing differential expression in the 21 *agl16-1* DEGs.
293 Moreover, we identified more than a quarter of up-regulated DEGs in the *agl16*
294 *soc1* line (77 among 286) being AGL16 targets in contrast to about 13.3% of
295 up-regulated DEGs in the *soc1-2* mutant (29 among 218; Yate's *chi-square*
296 *test*, $p = 0.0035$; Fig. 7E). Among the 67 up-regulated DEGs shared between
297 the *soc1-2* and *agl16 soc1* mutants, 18 (26.9%) were potentially AGL16
298 targets. In contrast, less than 8% of down-regulated DEGs in both mutants
299 were targeted by AGL16. Together, these data suggest that AGL16 may act
300 mainly as a transcriptional repressor and exert an antagonistic role against
301 SOC1 regulation on target gene expression.

302 **AGL16-SOC1 module is important for flowering time regulation**

303 Among the DEGs between *agl16 soc1* and *soc1-2* plants, we identified 17
304 known genes involved in floral regulation with seven being targeted by AGL16
305 (*NF-YA2*, *TCP21*, *RHL41*, *AGL16*, three *AP2-like* genes *RAV1*, *RAV2/TEM2*,
306 and *SNZ*; Fig. 7F; Table S4). Expression of *FT* was significantly enhanced in
307 the *agl16 soc1* double mutant. In line with this, the double mutant *agl16 soc1*
308 flowered significantly earlier (~20 rosette leaves) than the *soc1-2* single mutant
309 (~25.6 rosette leaves; about 21.6% reduction in rosette leaf number) but still
310 later than both *agl16-1* (~11.1 rosette leaves; ~13.6% reduction) and wild type
311 Col-0 (~12.9 rosette leaves) plants (Fig. 8). This indicated that *AGL16* could
312 counteract the *SOC1* regulation on flowering, while the regulatory role of
313 *AGL16* in floral transition depends on *SOC1*, a pattern like the genetic
314 dependency of *AGL16* on *FLC* (Hu et al., 2014).

315 **Discussion**

316 **AGL16 acts in the hubs of GRN related to various biological processes**

317 The MADS-box TF AGL16 is an important regulator in flowering time (Hu et al.,
318 2014), stomata development (Kutter et al., 2007), heat stress adaptation
319 (Szaker et al., 2019), drought resistance (Zhao et al., 2020) and salt stress
320 adaptation (Zhao et al., 2021), suggesting that it might have very broad
321 spectra of downstream targets. In this study, indeed, our ChIP-seq assay
322 demonstrated that AGL16 could target more than 2000 genes featuring
323 characteristic CArG-box motifs (Figs. 1-3). These genes were involved not
324 only plant development but also various hormone signaling processes (Table
325 S2) including some targets in the ABA signaling pathway that previously
326 identified (Zhao et al., 2020; Zhao et al., 2021). These broad spectra are not
327 rare, however, especially for MADS-box TFs. Two such examples would be
328 SVP and SEP3, both of which can bind to thousands of downstream targets
329 involved in a very broad set of biological processes (Kaufmann et al., 2009;
330 Gregis et al., 2013; Mateos et al., 2015). Intriguingly, both SVP and SEP3 can

331 or potentially form hetero-protein-complexes with AGL16 (de Folter et al., 2005;
332 Hu et al., 2014), indicating that they may work together to fine-tune plant
333 developmental programs in responding to ever-changing environments, a
334 hypothesis awaits for further investigation.

335 Interestingly, expression of AGL16 responds to ABA treatment as well as
336 multiple stresses (Szaker et al., 2019; Zhao et al., 2021), thus revealing a very
337 complex role of AGL16 (and its potential partners) in abiotic adaptation. Since
338 both AGL16 and SOC1 play important roles in stomata development and
339 movement (Kutter et al., 2007; Zhao et al., 2020), it's likely that the
340 hetero-protein-complexes formed between AGL16 and its partners may be the
341 key molecule that functions in these abiotic adaptations. Indeed, both AGL16
342 and SOC1 can directly bind and regulate the expression of a shared set of
343 genes involved in ABA signaling and abiotic stresses (Fig. 6) (Immink et al.,
344 2012; Tao et al., 2012). Considering the essential roles of ABA in seed
345 dormancy and germination regulation, the fact that several AGL16 targets
346 encode for ABA receptors may invoke us to further examine the regulatory
347 roles of AGL16 and its related protein complexes in seed dormancy and
348 germination (Table S2, S3). Corroborating with this, *AGL16* expression drops
349 substantially during seed germination (Das et al., 2018).

350 **AGL16 regulates multiple floral pathways**

351 AGL16 might exert its regulation potential in several pathways controlling
352 flowering time (Fig. 3). Being congruent with its photoperiod dependency in
353 regulation of flowering time, AGL16 targets 37 genes (including *AGL16* itself)
354 related to photoperiod and circadian clock pathways. Though under the tested
355 environmental conditions *ag/16-1* still shows a normal vernalization response
356 (Hu et al., 2014), several genes related to temperature responses are directly
357 targeted by AGL16. FLC, SVP and SOC1 might be partners of AGL16 in this
358 respect as all three proteins target also directly on some of these
359 temperature-related genes (Deng et al., 2011; Immink et al., 2012; Tao et al.,
360 2012; Mateos et al., 2015). The binding of AGL16 may cause both positive and

361 negative influences on the transcription of these targets (Fig. 7), which
362 encompass both repressors and promoters of the floral transition. Indeed,
363 several of the flowering time genes targeted by AGL16 show an enhanced or
364 decreased expression when *AGL16* activity is modified in the *soc1-2*
365 background (Fig. 3 and 7; Table S3, S4). Therefore, the early flowering
366 phenotypes present in *AGL16* loss-of-function mutants might be a net-effect or
367 balanced regulation on different pathways (Fig. 8) (Hu et al., 2014).

368 It should be noted that AGL16 also targets and represses the expression of
369 *MYC2*, which is previously claimed to modulate flowering time (Kazan and
370 Manners, 2013; Zhai et al., 2015; Wang et al., 2017; Bao et al., 2019).
371 However, our recent efforts have demonstrated, partially based on the data
372 generated from this study, that the MYC2-family TFs only play very limited
373 roles in timing floral transition, because it's the hidden mutation of *COP1*, not
374 the *MYC* mutations, causing early flowering observed in the original *jin1-2*
375 mutant (Yu et al., 2022). Whether the *AGL16-MYC2* interaction regulates
376 flowering time upon different stress conditions needs to be tested later.

377 **AGL16 and SOC1 collaborate in regulation of genome-wide gene** 378 **expression**

379 The formation of AGL16-SOC1 complex identifies the collaborative potential in
380 targeting and regulation of genome-wide gene expression like other
381 MADS-box TFs (Fig. 5) (de Folter et al., 2005; Lee et al., 2008; Immink et al.,
382 2009; Kaufmann et al., 2009; Kaufmann et al., 2010; Deng et al., 2011; Immink
383 et al., 2012; Tao et al., 2012; Mateos et al., 2015). AGL16 binds more than
384 2000 genes, which is in line with its very broad expression in many tissues and
385 organs (Alvarez-Buylla et al., 2000), but affects the expression of a very limited
386 number of genes in the background of Col-0 (Fig. 7). When *SOC1* becomes
387 non-functional (*soc1-2*), AGL16 modulates the expression of more than 550
388 genes and acts both as a transcriptional repressor and activator. In the *soc1-2*
389 background, AGL16 seems mainly act as a transcriptional repressor as more
390 than a quarter of the up-regulated DEGs, in contrast to the less than 8.5% of

391 the down-regulated DEGs, are potential targets of AGL16. Hence AGL16's
392 activity in gene expression regulation requires partially SOC1, and
393 corroborating with this, both *AGL16* and *SOC1* expression can be detected in
394 the shoot apex (Corbesier et al., 2007; Immink et al., 2012; Hu et al., 2014).
395 On the other hand, SOC1 also needs *AGL16* as SOC1's repressive activity
396 substantially drops (from 155 to 49 genes) but the promoting activity increases
397 (from 285 to 353 genes) when *AGL16* has no function. Many *soc1-2* DEGs are
398 not differentially expressed any more in *agl16 soc1* mutant (Fig. 7). Indeed,
399 AGL16 and SOC1 co-bind a common set of targets and regulate the
400 expression of many known flowering time genes (Fig. 6, 7). As expected, these
401 two TFs collaborate in regulation of flowering time (Fig. 8). The *agl16 soc1*
402 double mutant flowered significantly earlier than the *soc1-2* single mutant, on
403 the other hand, still later than both *agl16-1* and wild type plants. *AGL16* could
404 counteract *SOC1* effects in flowering time regulation, and vice versa, similar to
405 the genetic dependency of *AGL16* on *FLC* (Hu et al., 2014). It's possible that
406 these TFs may form higher-order protein complexes to regulate downstream
407 genes, for example *FT* expression, which should be tested further.

408 The identification of three DNA fragments bound by AGL16 in the upstream ~4
409 Kb intergenic region raises a possibility that the *SOC1* expression regulation
410 might be more complicated than we have expected (Fig. 4) (Hepworth et al.,
411 2002; Immink et al., 2012; Jung et al., 2012; Liu et al., 2013; Li et al., 2017;
412 Hwang et al., 2019; Olas et al., 2019; Yan et al., 2021). Though AGL16 can
413 repress the *SOC1* expression in planta and when the frequently used ~1.7 Kb
414 promoter was included in transient assays (Fig. 4), this short fragment may not
415 be enough for full mechanistic understanding the regulation of *SOC1*
416 expression. Whether higher order 3D chromatin loop presents for *SOC1*, like
417 the ones for *FT* and *FLC* (Crevillen et al., 2013; Liu et al., 2014), and whether
418 AGL16 has a role in the loop formation need further investigation.

419 Together, as a master regulator in GRNs connecting multiple pathways,
420 AGL16's function has a partial inter-dependency with SOC1. AGL16 might act
421 as a glue molecule, like other MADS-box TFs do, to micro-tune the expression
422 of downstream genes at proper stages and environmental conditions (Immink

423 et al., 2009; Kaufmann et al., 2010; Pajoro et al., 2014; Richter et al., 2019). It
424 will be important to address these further to understand their precise roles and
425 mechanisms in balancing development and environmental adaptation.

426 **Materials and Methods**

427 **Plant materials, growth conditions, and phenotype assays**

428 *Arabidopsis thaliana* plants including wild-type Col-0, *agl16-1*,
429 *35S:AGL16-YFP-HA* in *agl16-1* background, Col-*FRI*, *agl16-1* Col-*FRI*, and
430 *m3* have been described previously (Kutter et al., 2007; Hu et al., 2014). The
431 *soc1-2* mutant in Col-0 background (Torti et al., 2012) was kindly provided by
432 Prof. George Coupland. To test the genetic interactions between *AGL16* and
433 *SOC1*, *agl16-1* and *soc1-2* were crossed and double mutant was screened
434 with gene-specific primers (Table S5) (Kutter et al., 2007; Torti et al., 2012; Hu
435 et al., 2014).

436 *Arabidopsis* seeds were stratified in distilled water at 4°C for 72 h and sown in
437 soil and grown under LD conditions (16-h light at 21°C and 8-h night at 18°C).
438 Seedlings for phenotyping were planted either in growth rooms or chambers,
439 while materials for gene expression analysis and ChIP assays were sown on
440 Murashige and Skoog medium plates (Hu et al., 2014).

441 Flowering time assays were carried out according to previous report (Hu et al.,
442 2014). Four independent trials were applied and each gave similar pattern.
443 Phenotype comparisons were performed with Student's *t*-test with
444 *Bonferroni-correction*.

445 **RNA Isolation, RT-qPCR, and RNA-seq assays**

446 Total RNA was extracted with TRI Reagent[®] (Molecular Research Center, Inc.
447 Cincinnati, USA). Ten days old seedlings were used for quantification of relative
448 expression of selected genes with *PP2A* as reference (Hu et al., 2014).

449 Reverse transcription was carried out with the HiScript[®] II Q RT SuperMix for
450 RT-qPCR (+gDNA wiper) and quantification PCRs were performed with
451 ChamQ[™] SYBR qPCR Master Mix (both from Vazyme Biotech co. Ltd, Nanjing)
452 on QuantStudio[™] 7 Flex Real-Time PCR System (ThermoFisher). Three to
453 four biological replicates from each of two to three independent trials were
454 applied for each experiment. A similar protocol was developed for monitoring
455 relative enrichment of DNA fragments in ChIP-qPCR experiments. All the
456 primers used in this study are included in Table S1.

457 For RNA-seq, materials were collected from three independent biological
458 replicates for each genotype, and DNA-free total RNA was generated as
459 described above. Illumina True-seq library preparation was performed from 3
460 µg DNA-free total RNA and sequenced by the Biomarker Technologies
461 Corporation, Beijing, China. Quality trimmed pair-end RNA-seq reads were
462 mapped to the Arabidopsis TAIR10 annotation using the *HISAT2* v2.1.0 (Kim
463 et al., 2019). The *featureCounts* included in *subread* v1.6.4 package was
464 applied to calculate reads counts on each gene (Liao et al., 2013; Liao et al.,
465 2014). *DESeq2* v1.14.1 was used to detect differentially expressed genes
466 (DEGs; fold change above 1.5 and p.adj<0.1). Only uniquely mapped reads
467 were used for downstream analysis. Transcriptional clustering analysis was
468 performed using the *heatmap.2* function in *R*. GO analysis was performed with
469 *PANTHER* in TAIR web-tool ([https://www.arabidopsis.org/tools/
470 go_term_enrichment.jsp](https://www.arabidopsis.org/tools/go_term_enrichment.jsp)) or *agriGO* pipeline (Mi et al., 2017; Tian et al., 2017).

471 **ChIP-seq, ChIP-qPCR assays and data analysis**

472 ChIP experiments were carried out following protocols described (Reimer and
473 Turck, 2010; Zhou et al., 2016). Chromatin for both *agl16-1* and *agl16-1*
474 *AGL16OX* plants was extracted from ten-day-old seedlings grown under LD
475 conditions at ZT14, and precipitated with antibody against GFP (Abcam,
476 Ab290). For ChIP-seq, the immuno-precipitations from two independent trials
477 were used for NGS library preparation with NEBNext[®] Ultra[™] II DNA Library
478 Prep Kit for Illumina[®] (E7645, New England BioLabs Inc.) and high-throughput

479 sequencing with HiSeq2000 platform. ChIP-seq reads were mapped to the
480 TAIR10 assembly of *A. thaliana* using *BWA-MEM* (v0.7.17-r1188) (Li, 2013).
481 Reads with mapping quality below 30 were discarded with *SAMtools* v1.7 (Li et
482 al., 2009). Duplicated reads were removed using *Picard MarkDuplicates*
483 v1.119. The resulted *.bam* file was used as input to call AGL16 enriched
484 regions with *MACS* v2.2.7.1 (Zhang et al., 2008). Enriched regions were
485 generated by the comparison of immune-precipitated products to input for
486 *AGL16OX* and then compared against *agl16-1*. For annotation of AGL16
487 targets, the *R* package *ChIPseeker* was used (Yu et al., 2015). The position
488 and strand information of nearest genes were reported with the distance from
489 peak to the TSS of its closest gene identified. As annotations might
490 overlap, we use 'promoter' definition in *ChIPseeker* as the highest priority for
491 annotation. Each binding site was assigned to only one gene. IGV was used
492 for data visualization of the binding profiles for targets (Thorvaldsdottir et al.,
493 2013). Enriched motifs in AGL16 binding peaks were identified using *Homer*
494 suite with *findMotifsGenome.pl* function (Heinz et al., 2010). Motifs in
495 AGL16-SOC1 co-targeted regions were analyzed with *MEME-ChIP* tools
496 (Machanick and Bailey, 2011), and the spacing between primary and
497 secondary motifs was analyzed with *SpaMo* (*spamo -dumpseqs -bin 20*
498 *-verbosity 1 -oc spamo_out_1 -bgfile./background -keepprimary -primary*
499 *DCCAAAAWGGAAAR*). We compared the AGL16 targets to SOC1 targets
500 from both Immink (2012) and Tao (2012) with the same annotation procedures
501 for AGL16 (Immink et al., 2012; Tao et al., 2012). In an earlier independent trial,
502 we pooled the immuno-precipitations from two biological replicates and
503 sequenced the products. This pooled sequencing results gave similar pattern
504 of AGL16 targets profile but with a lower coverage. *Yate's chi-square tests*
505 were performed online (<http://www.quantpsy.org/chisq/chisq.htm>). The ~400
506 flowering time genes were downloaded from <https://www.mpipz.mpg.de>
507 (Bouche et al., 2016) with self-curations. Reads data for RNA-seq and
508 ChIP-seq experiments were accessible at NCBI under accession code
509 SUB5067038.

510 **Yeast two-hybrid and biomolecular fluorescence complementation (BiFC)**
511 **experiments**

512 Yeast two-hybrid and the BiFC assays were carried out to test the physical
513 interaction between AGL16 and SOC1 proteins according to previous report
514 (Hu et al., 2014). In yeast two-hybrid assay, interactions between AGL16-SVP
515 and AGL16-AGL16 were applied as positive controls while the AGL16-LHP1,
516 AGL16-BD, SOC1-BD, AD-AGL16, and AD-SOC1 were applied as negative
517 controls together with empty vectors. For BiFC assay in *Nicotiana*
518 *benthamiana* plants, 35S:SOC1-cYFP construct was built by cloning the
519 full-length encoding-region without stop codon of SOC1 (from Col-0) into
520 pDONR221 entry vector first and later transferred into RfA-sYFPc-pBatTL-B
521 vector. The interactions between AGL16 and SVP, between AGL16 and LHP1,
522 were used as positive and negative controls, respectively.

523 **Co-immunoprecipitation (co-IP) assay**

524 To test the AGL16 and SOC1 interactions, coding sequences of AGL16 and
525 SOC1 were amplified from the wild type cDNA with Phanta Max Super-Fidelity
526 DNA Polymerase (P505, Vazyme). All sequences were cloned into the
527 pDONR201 entry vector and verified via Sanger sequencing. The resulting
528 destination vectors containing N-terminal tagged pENSG-YFP-AGL16 and
529 pICH47811-SOC1 were used to transfect protoplasts prepared from leaves of
530 wild type seedlings (Yoo et al., 2007). The transfected protoplasts were
531 incubated at room temperature for 16 hr and used for co-IP assays as
532 described previously (Cui et al., 2018). In brief, the protoplasts were lysed in
533 immunoprecipitation buffer (50 mM Tris pH7.5, 150 mM NaCl, 10 % (v/v)
534 glycerol, 2 mM EDTA, 5 mM DTT, protease inhibitor, 0.1% Triton). Lysates
535 were centrifuged at 14000 × g for 15 min at 4 °C with aliquots of supernatants
536 as input controls. Immunoprecipitations (IPs) were performed by incubating
537 the supernatants with 15 μL GFP-Trap beads (gta-10, ChromoTek) for 2 h at
538 4 °C. After centrifugation at 1000 × g and washing four times with extraction
539 buffer, beads were eluted with 2× Laemmli loading buffer. The proteins were
540 then separated with SDS-PAGE and analyzed by immuno-blotting with
541 antibodies against GFP (ab290, Abcam) and FLAG (ab49763, Abcam).

542 **Transient transactivation assay**

543 To test the regulatory effects of AGL16 on *SOC1* expression, the coding region
544 of *AGL16* was inserted into the *pOCA30* vector to generate the effector, while
545 the 1.7 Kb promoter and its mutated versions of *SOC1* was fused with a *pZP*
546 vector to generate the reporter constructs (Chen et al., 2021). Equal amounts
547 of the effector and reporter constructs in *Agrobacterium tumefaciens* strain
548 GV3101 were used to co-infiltrate *N. benthamiana* leaves with at least 15
549 biological replicates that were randomly distributed. After two days of
550 infiltration, the luciferase intensity was collected and quantified with a low-light
551 cooled CCD imaging apparatus. Experiments were triplicated with each
552 containing at least 15 replicates. Relative expression was examined for
553 statistical significance using ANOVA followed by Dunnett's test.

554 **Accession Numbers**

555 Sequence data from this article can be found in the CNSA database
556 (<https://db.cngb.org/>) under project number CNP0003940.

557

558

559

560

561

562

563

564

565

566

567

568

569

570

571

572

573

574

575

576

577 **Funding information**

578 This work was supported by grants from the National Natural Science
579 Foundation of China (31570311 to J-Y H, 31501034 to X D, 31700275 to Y-X D,
580 31800261 to F C), the Strategic Priority Research Program of the Chinese
581 Academy of Sciences (CAS) to J-Y H (XDB31000000), the China Postdoctoral
582 Science Foundation (2017M613023 to Y-X D), the Postdoctoral targeted
583 funding from Yunnan Province to F C and Y-X D, the CAS Pioneer Hundred
584 Talents Program (292015312D11035 to J-Y H), and the Yunnan basic and
585 applied research funding to F C. This work is partially facilitated by the
586 Germplasm Bank of Wild Species of China and the Platform for Plant
587 Multi-dimensional Imaging and Diversity Analysis.

588 **Acknowledgments**

589 We thank Franziska Turck, Ligang Chen, Liangyu Liu, Feihong Yan, Fei He,
590 Yibo Sun, Shulan Chen, and Zhijia Gu for insightful discussion and assistance
591 in experiments.

592 **Conflict of interest statement**

593 The authors declare no competing interests.

594 **Data and materials availability**

595 All data and materials needed to evaluate the conclusions in the paper are
596 present in the paper and the Supplementary materials.

597 **Figure legends**

598

599 **Fig. 1 Validation of the AGL16 binding on target DNA fragments.**

600 **A.** Binding profiles for selected target genes. The TAIR10 annotation of the
601 genomic locus was shown at the bottom of each box. For each panel, the
602 profiles for two trials (R1 and R2) in *agl16-1* background line were shown in the
603 upper panel, while the profiles for *agl16-1 35S:AGL16-YFP-HA (AGL16OX;*
604 *two trials)* were shown in the middle panel of each box. All the genes were
605 from 5'-end to 3'-end with scale bars indicating sequence lengths of 500 bp.
606 Note that data range for each gene in *agl16-1* and *AGL16OX* was the same
607 scale, but different genes could have different scale. Red lines marked the
608 binding regions tested via ChIP-qPCR assays (**B**).

609 **B.** ChIP-qPCR validation of AGL16 binding on 20 DNA segments. Significant
610 enrichment (red bars) was defined with the following criteria: mean enrichment
611 must be at least two-fold higher than negative control *ACT7*, the enrichment for
612 *AGL16OX* (in *agl16-1* background) than *agl16-1* must be higher than two-fold
613 change, and the amplification C_T number of IP samples must be at least two
614 cycles less than no-antibody controls. This experiment was repeated with
615 another independent trial, which gave similar pattern. Statistics was carried out
616 with *Student's t-test* with Bonferroni correction. ***, $P < 0.001$; **, $p < 0.01$; *,
617 $p < 0.05$.

618

619 **Fig. 2 Genome-wide identification of AGL16 target genes via ChIP-seq.**

620 **A.** Venn diagram of AGL16 targets identified in two independent trials.

621 **B.** Distribution of AGL16 binding sites for two trials surrounding the

622 transcriptional starting site (TSS).
623 **C.** Location distribution in relative to nearby genes for AGL16 binding sites of
624 trial 1. Peaks within the 3 Kb promoter region were taken as AGL16 targets.
625 **D.** CArG type of motifs over-represented in the AGL16 binding peaks. AGL16
626 new, which was highly similar to known SOC1 type, showed the *de novo* motif
627 predicted for AGL16. Frequency gave the percentage for each motif presented
628 in the binding peaks.
629 **E.** Distribution of new (orange) and known (gray; shown in **D**) CArG type of
630 motifs around AGL16 peaks center.

631

632 **Fig. 3 Molecular pathways (indicated with different color boxes) targeted**
633 **by AGL16.** Genes with names in bold were common targets for AGL16 and
634 SOC1, while those in red were differentially expressed between the *agl16 soc1*
635 and *soc1-2* mutants.

636

637 **Fig. 4 AGL16 targets SOC1 and represses its expression.**

638 **A.** Schematic representation of the *SOC1* locus. Filled bars indicated exons
639 and gray bars marked the 5'- and 3'-UTR regions while the line indicated the
640 non-coding region of *SOC1*. Arrows downward labelled the putative
641 CArG-boxes potentially bound by MADS-box proteins. The dark purple lines
642 indicated the three peaks (P1389, P1390 and P1391) bound by AGL16.
643 Orange, blue and black thick lines marked the known regions targeted by FLC,
644 SVP and SOC1, respectively. Note that two sites in the regulatory region of
645 *SOC1* were bound by itself (SOC1 binding R1 and R2; see ref. Tao et al. 2012).
646 Red lines (1 to 7) showed the regions tested for AGL16-YFP-HA binding on
647 *SOC1* chromatin. Horizontal arrows marked the position of primers used for
648 quantification of CDS regions. The lower panel showed the ChIP-seq profile at
649 *SOC1*.

650 **B.** Relative enrichment of AGL16 on *SOC1* chromatin tested with ChIP-qPCR.
651 Mean fold change values with significant enrichment was labelled above bars
652 together with standard deviation. *ACT7* was taken as a negative enrichment
653 control.

654 **C.** Relative expression of *SOC1* against *PP2A* in Col-0 and *agl16-1* plants.

655 Mean relative expression was given with standard deviation and the significant
656 difference was examined using Student's *t*-test.

657 **D.** Quantitative luciferase assay showing that AGL16 regulated the expression
658 of 1.7 Kb promoter of *SOC1* via *cis*-motifs 3,4,5,6 described in **A**. Box plots
659 mark the 25% to 75% quartiles with the line in box representing the median.
660 The lines extending from each box marked the minimum (5%) and maximum
661 (95%) values of the dataset. Circles showed the outliers. WT marked the 1.7
662 Kb promoter without any sequence modification, while the m3 indicated the
663 mutation of a CCW₆GG-box in WT background. The m3456 and m456 showed
664 the relative expression level for the WT promoter with *cis*-motifs 3,4,5,6 and
665 4,5,6 mutated, respectively. At least 15 randomly selected fields each from one
666 individual *N. benthamiana* leaf per treatment were used for measuring with +
667 and – labeling the presence and absence of 35S:AGL16, respectively.
668 Different letters above the boxes represented the significant differences among
669 treatments using one-way ANOVA Donnett's test ($P < 0.05$). This experiment
670 was triplicated and each trial gave similar results.

671

672 **Fig. 5 AGL16 forms protein complex with SOC1.**

673 **A.** Yeast two-hybrid assay revealed a direct interaction between AGL16 and
674 SOC1. Each protein was fused to either the activation domain (AD) as prey or
675 the DNA-binding domain (BD) as bait. Serial dilutions (10^0 x to 10^{-3} x) of J69-4A
676 cells containing different construct combinations indicated on the left were
677 grown on control (left) and selective (right) medium. The AGL16-SVP and the
678 AGL16-LHP1/empty vector combinations provided positive and negative
679 controls, respectively.

680 **B.** BiFC assay evidenced the formation of AGL16-SOC1 complex in nucleus of
681 *Nicotiana benthamiana* leaf epidermis. The interaction was tested with
682 constructs 35S:*SOC1-cYFP* and 35S:*AGL16-nYFP*. A negative interaction
683 between AGL16 and LHP1 and a positive interaction between AGL16 and SVP
684 were tested as well. Bars = 10 μ m.

685 **C.** Co-immunoprecipitation (co-IP) assay confirmed the AGL16-SOC1
686 interaction in Arabidopsis protoplast. SOC1 was FLAG-tagged while the
687 AGL16 was fused with a YFP tag. Total protein of the transfected wild type

688 protoplasts was immuno-precipitated with antibody against GFP (anti-GFP)
689 first, and further analyzed by Western blot using antibody against FLAG
690 (anti-FLAG).

691

692 **Fig. 6 AGL16 and SOC1 share a common set of target genes involved in**
693 **multiple functions.**

694 **A.** Venn diagram showing that 223/171 genes (Immink et al. 2012 / Tao et al.
695 2012) were co-bound potentially by both AGL16 and SOC1.

696 **B.** Binding intensities for AGL16 (red) and SOC1 (blue) peaks surrounding
697 transcription starting sites (TSS). Regions 3kb upstream and downstream of
698 TSS were plotted.

699 **C.** Selected significantly-enriched GO terms for the common targets.

700

701 **Fig. 7 The AGL16-SOC1 module collaborates on regulation of**
702 **genome-wide gene expression.**

703 **A.** The number of differentially expressed genes (DEGs) in three mutants. The
704 exact number of up (red) or down (blue) regulated DEGs were given on each
705 cone.

706 **B** and **C.** Heatmaps showing the normalized relative expression of *soc1-2* (**B**)
707 and *agl16 soc1* (**C**) DEGs in all four lines. The boxplots in the middle gave the
708 data distribution pattern for each cluster. Box plots mark the 25% to 75%
709 quartiles with the line in box representing the median. The lines extending from
710 each box marked the minimum (5%) and maximum (95%) values of the
711 dataset. Circles showed the outliers.

712 **D.** Venn diagram demonstrating the overlap between DEGs and the AGL16
713 targets profile.

714 **E.** A detailed comparison between the DEGs in *soc1-2* and *agl16 soc1*
715 mutants with the AGL16 binding profile. Bold numbers in brackets showed the
716 number of DEGs bound by AGL16.

717 **F.** A heatmap showing the normalized relative expression of the DEGs related
718 to flowering time regulation in the *soc1-2* and *agl16 soc1* mutants.

719

720 **Fig. 8 AGL16 and SOC1 regulate additively flowering time.**

721 **A.** Overall flowering behaviors of LD-growing wild type Col-0, *agl16-1*, *soc1-2*
722 and *agl16 soc1* mutants.

723 **B.** Leaf number production upon flowering under LD conditions. Mean rosette
724 (filled bars, RLN) and cauline (open bars, CLN) leaves were shown with
725 standard deviation. Numbers in percentage showed the earlier flowering level
726 of *agl16-1* and *agl16 soc1* comparing to Col-0 and *soc1-2*, respectively.
727 Analyses were triplicated and all had similar patterns. Statistical comparisons
728 were performed with *Wilcoxon rank sum test* in *R*.

729

730 **References**

731 **Aerts N, de Bruijn S, van Mourik H, Angenent GC, van Dijk ADJ** (2018) Comparative
732 analysis of binding patterns of MADS-domain proteins in *Arabidopsis thaliana*. *BMC Plant*
733 *Biology* **18**: 131

734 **Alvarez-Buylla ER, Liljegren SJ, Pelaz S, Gold SE, Burgeff C, Ditta GS, Vergara-Silva F,**
735 **Yanofsky MF** (2000) MADS-box gene evolution beyond flowers: expression in pollen,
736 endosperm, guard cells, roots and trichomes. *Plant J* **24**: 457-466

737 **Andres F, Coupland G** (2012) The genetic basis of flowering responses to seasonal cues.
738 *Nat Rev Genet* **13**: 627-639

739 **Aukerman MJ, Sakai H** (2003) Regulation of flowering time and floral organ identity by a
740 MicroRNA and its APETALA2-like target genes. *Plant Cell* **15**: 2730-2741

741 **Bao S, Hua C, Huang G, Cheng P, Gong X, Shen L, Yu H** (2019) Molecular Basis of Natural
742 Variation in Photoperiodic Flowering Responses. *Developmental Cell* **50**: 90-101.e103

743 **Bouche F, Lobet G, Tocquin P, Perilleux C** (2016) FLOR-ID: an interactive database of
744 flowering-time gene networks in *Arabidopsis thaliana*. *Nucleic Acids Research* **44**:
745 D1167-D1171

746 **Boxall SF, Foster JM, Bohnert HJ, Cushman JC, Nimmo HG, Hartwell J** (2005)
747 Conservation and Divergence of Circadian Clock Operation in a Stress-Inducible
748 Crassulacean Acid Metabolism Species Reveals Clock Compensation against Stress.
749 *Plant Physiology* **137**: 969-982

750 **Castillejo C, Pelaz S** (2008) The balance between CONSTANS and TEMPRANILLO activities

751 determines FT expression to trigger flowering. *Curr Biol* **18**: 1338-1343

752 **Chen Y, Zhang L, Zhang H, Chen L, Yu D** (2021) ERF1 delays flowering through direct
753 inhibition of FLOWERING LOCUS T expression in Arabidopsis. *J Integr Plant Biol* **63**:
754 1712-1723

755 **Corbesier L, Vincent C, Jang S, Fornara F, Fan Q, Searle I, Giakountis A, Farrona S,**
756 **Gissot L, Turnbull C, Coupland G** (2007) FT protein movement contributes to
757 long-distance signaling in floral induction of Arabidopsis. *Science* **316**: 1030-1033

758 **Crevillen P, Sonmez C, Wu Z, Dean C** (2013) A gene loop containing the floral repressor FLC
759 is disrupted in the early phase of vernalization. *EMBO J* **32**: 140-148

760 **Cui HT, Qiu JD, Zhou Y, Bhandari DD, Zhao CH, Bautor J, Parker JE** (2018) Antagonism of
761 Transcription Factor MYC2 by EDS1/PAD4 Complexes Bolsters Salicylic Acid Defense in
762 Arabidopsis Effector-Triggered Immunity. *Molecular Plant* **11**: 1053-1066

763 **Das SS, Yadav S, Singh A, Gautam V, Sarkar AK, Nandi AK, Karmakar P, Majee M,**
764 **Sanan-Mishra N** (2018) Expression dynamics of miRNAs and their targets in seed
765 germination conditions reveals miRNA-ta-siRNA crosstalk as regulator of seed germination.
766 *Scientific Reports* **8**: 13

767 **de Folter S, Immink RG, Kieffer M, Parenicova L, Henz SR, Weigel D, Busscher M,**
768 **Kooiker M, Colombo L, Kater MM, Davies B, Angenent GC** (2005) Comprehensive
769 interaction map of the Arabidopsis MADS Box transcription factors. *Plant Cell* **17**:
770 1424-1433

771 **de Meaux J, Hu JY, Tartler U, Goebel U** (2008) Structurally different alleles of the
772 ath-MIR824 microRNA precursor are maintained at high frequency in Arabidopsis thaliana.
773 *Proc Natl Acad Sci U S A* **105**: 8994-8999

774 **Deng W, Ying H, Helliwell CA, Taylor JM, Peacock WJ, Dennis ES** (2011) FLOWERING
775 LOCUS C (FLC) regulates development pathways throughout the life cycle of Arabidopsis.
776 *Proc Natl Acad Sci U S A* **108**: 6680-6685

777 **Fahlgren N, Howell MD, Kasschau KD, Chapman EJ, Sullivan CM, Cumbie JS, Givan SA,**
778 **Law TF, Grant SR, Dangl JL, Carrington JC** (2007) High-throughput sequencing of
779 Arabidopsis microRNAs: evidence for frequent birth and death of MIRNA genes. *PLoS One*
780 **2**: e219

781 **Fornara F, de Montaigu A, Coupland G** (2010) SnapShot: Control of flowering in Arabidopsis.
782 *Cell* **141**: 550, 550 e551-552

783 **Gregis V, Andres F, Sessa A, Guerra R, Simonini S, Mateos J, Torti S, Zambelli F,**

784 **Prazzoli G, Bjerkan K, Grini P, Pavesi G, Colombo L, Coupland G, Kater M** (2013)
785 Identification of pathways directly regulated by SHORT VEGETATIVE PHASE during
786 vegetative and reproductive development in Arabidopsis. *Genom Biol* **14**: R56

787 **Heinz S, Benner C, Spann N, Bertolino E, Lin YC, Laslo P, Cheng JX, Murre C, Singh H,**
788 **Glass CK** (2010) Simple Combinations of Lineage-Determining Transcription Factors
789 Prime cis-Regulatory Elements Required for Macrophage and B Cell Identities. *Molecular*
790 *Cell* **38**: 576-589

791 **Hepworth SR, Valverde F, Ravenscroft D, Mouradov A, Coupland G** (2002) Antagonistic
792 regulation of flowering-time gene SOC1 by CONSTANS and FLC via separate promoter
793 motifs. *EMBO J* **21**: 4327-4337

794 **Hu JY, Zhou Y, He F, Dong X, Liu LY, Coupland G, Turck F, de Meaux J** (2014)
795 miR824-Regulated AGAMOUS-LIKE16 Contributes to Flowering Time Repression in
796 Arabidopsis. *Plant Cell* **26**: 2024-2037

797 **Hwang K, Susila H, Nasim Z, Jung J-Y, Ahn JH** (2019) Arabidopsis ABF3 and ABF4
798 Transcription Factors Act with the NF-YC Complex to Regulate SOC1 Expression and
799 Mediate Drought-Accelerated Flowering. *Molecular Plant* **12**: 489-505

800 **Hyun Y, Richter R, Vincent C, Martinez-Gallegos R, Porri A, Coupland G** (2016)
801 Multi-layered Regulation of SPL15 and Cooperation with SOC1 Integrate Endogenous
802 Flowering Pathways at the Arabidopsis Shoot Meristem. *Developmental Cell* **37**: 254-266

803 **Immink RG, Tonaco IA, de Folter S, Shchennikova A, van Dijk AD, Busscher-Lange J,**
804 **Borst JW, Angenent GC** (2009) SEPALLATA3: the 'glue' for MADS box transcription factor
805 complex formation. *Genome Biol* **10**: R24

806 **Immink RGH, Posé D, Ferrario S, Ott F, Kaufmann K, Valentim FL, de Folter S, van der**
807 **Wal F, van Dijk ADJ, Schmid M, Angenent GC** (2012) Characterization of SOC1's Central
808 Role in Flowering by the Identification of Its Upstream and Downstream Regulators. *Plant*
809 *Physiology* **160**: 433-449

810 **Johanson U, West J, Lister C, Michaels S, Amasino R, Dean C** (2000) Molecular Analysis
811 of FRIGIDA, a Major Determinant of Natural Variation in Arabidopsis Flowering Time.
812 *Science* **290**: 344-347

813 **Jung JH, Ju Y, Seo PJ, Lee JH, Park CM** (2012) The SOC1-SPL module integrates
814 photoperiod and gibberellic acid signals to control flowering time in Arabidopsis. *Plant J* **69**:
815 577-588

816 **Jung JH, Seo YH, Seo PJ, Reyes JL, Yun J, Chua NH, Park CM** (2007) The

817 GIGANTEA-regulated microRNA172 mediates photoperiodic flowering independent of
818 CONSTANS in Arabidopsis. *Plant Cell* **19**: 2736-2748

819 **Kaufmann K, Muino JM, Jauregui R, Airoidi CA, Smaczniak C, Krajewski P, Angenent**
820 **GC** (2009) Target genes of the MADS transcription factor SEPALLATA3: integration of
821 developmental and hormonal pathways in the Arabidopsis flower. *PLoS Biol* **7**: e1000090

822 **Kaufmann K, Wellmer F, Muino JM, Ferrier T, Wuest SE, Kumar V, Serrano-Mislata A,**
823 **Madueno F, Krajewski P, Meyerowitz EM, Angenent GC, Riechmann JL** (2010)
824 Orchestration of floral initiation by APETALA1. *Science* **328**: 85-89

825 **Kazan K, Manners JM** (2013) MYC2: The Master in Action. *Molecular Plant* **6**: 686-703

826 **Kim D, Paggi JM, Park C, Bennett C, Salzberg SL** (2019) Graph-based genome alignment
827 and genotyping with HISAT2 and HISAT-genotype. *Nature Biotechnology* **37**: 907-+

828 **Kutter C, Schob H, Stadler M, Meins F, Jr., Si-Ammour A** (2007) MicroRNA-mediated
829 regulation of stomatal development in Arabidopsis. *Plant Cell* **19**: 2417-2429

830 **Lee J, Lee I** (2010) Regulation and function of SOC1, a flowering pathway integrator. *Journal*
831 *of Experimental Botany* **61**: 2247-2254

832 **Lee J, Oh M, Park H, Lee I** (2008) SOC1 translocated to the nucleus by interaction with
833 AGL24 directly regulates leafy. *Plant J* **55**: 832-843

834 **Li D, Liu C, Shen L, Wu Y, Chen H, Robertson M, Helliwell CA, Ito T, Meyerowitz E, Yu H**
835 (2008) A repressor complex governs the integration of flowering signals in Arabidopsis. *Dev*
836 *Cell* **15**: 110-120

837 **Li H** (2013) Aligning sequence reads, clone sequences and assembly contigs with BWA-MEM.
838 arXiv: 1303.3997

839 **Li H, Handsaker B, Wysoker A, Fennell T, Ruan J, Homer N, Marth G, Abecasis G, Durbin**
840 **R, Genome Project Data P** (2009) The Sequence Alignment/Map format and SAMtools.
841 *Bioinformatics* **25**: 2078-2079

842 **Li H, Ye K, Shi Y, Cheng J, Zhang X, Yang S** (2017) BZR1 Positively Regulates Freezing
843 Tolerance via CBF-Dependent and CBF-Independent Pathways in Arabidopsis. *Molecular*
844 *Plant* **10**: 545-559

845 **Liao Y, Smyth GK, Shi W** (2013) The Subread aligner: fast, accurate and scalable read
846 mapping by seed-and-vote. *Nucleic Acids Research* **41**

847 **Liao Y, Smyth GK, Shi W** (2014) featureCounts: an efficient general purpose program for
848 assigning sequence reads to genomic features. *Bioinformatics* **30**: 923-930

849 **Liu L, Adrian J, Pankin A, Hu J, Dong X, von Korff M, Turck F** (2014) Induced and natural

850 variation of promoter length modulates the photoperiodic response of FLOWERING
851 LOCUS T. *Nat Commun* **5**

852 **Liu T, Li Y, Ren J, Qian Y, Yang X, Duan W, Hou X** (2013) Nitrate or NaCl regulates floral
853 induction in *Arabidopsis thaliana*. *Biologia* **68**: 215-222

854 **Machanick P, Bailey TL** (2011) MEME-ChIP: motif analysis of large DNA datasets.
855 *Bioinformatics* **27**: 1696-1697

856 **Mateos J, Madrigal P, Tsuda K, Rawat V, Richter R, Romera-Branchat M, Fornara F,**
857 **Schneeberger K, Krajewski P, Coupland G** (2015) Combinatorial activities of SHORT
858 VEGETATIVE PHASE and FLOWERING LOCUS C define distinct modes of flowering
859 regulation in *Arabidopsis*. *Genome Biology* **16**: 31

860 **Mateos JL, Tilmes V, Madrigal P, Severing E, Richter R, Rijkenberg CWM, Krajewski P,**
861 **Coupland G** (2017) Divergence of regulatory networks governed by the orthologous
862 transcription factors FLC and PEP1 in Brassicaceae species. *Proc Natl Acad Sci U S A* **114**:
863 E11037-E11046

864 **Mathieu J, Yant LJ, Murdter F, Kuttner F, Schmid M** (2009) Repression of flowering by the
865 miR172 target SMZ. *PLoS Biol* **7**: e1000148

866 **Mi HY, Huang XS, Muruganujan A, Tang HM, Mills C, Kang D, Thomas PD** (2017)
867 PANTHER version 11: expanded annotation data from Gene Ontology and Reactome
868 pathways, and data analysis tool enhancements. *Nucleic Acids Research* **45**: D183-D189

869 **Michaels SD** (2009) Flowering time regulation produces much fruit. *Curr Opin Plant Biol* **12**:
870 75-80

871 **Michaels SD, Amasino RM** (2001) Loss of FLOWERING LOCUS C activity eliminates the
872 late-flowering phenotype of FRIGIDA and autonomous pathway mutations but not
873 responsiveness to vernalization. *Plant Cell* **13**: 935-941

874 **Nee G, Xiang Y, Soppe WJJ** (2017) The release of dormancy, a wake-up call for seeds to
875 germinate. *Current Opinion in Plant Biology* **35**: 8-14

876 **Olas JJ, Van Dingenen J, Abel C, Dzialo MA, Feil R, Krapp A, Schlereth A, Wahl V** (2019)
877 Nitrate acts at the *Arabidopsis thaliana* shoot apical meristem to regulate flowering time.
878 *The New phytologist* **223**: 814-827

879 **Pajoro A, Madrigal P, Muiño JM, Matus JT, Jin J, Mecchia MA, Debernardi JM, Palatnik**
880 **JF, Balazadeh S, Arif M, Ó'Maoiléidigh DS, Wellmer F, Krajewski P, Riechmann J-L,**
881 **Angenent GC, Kaufmann K** (2014) Dynamics of chromatin accessibility and gene
882 regulation by MADS-domain transcription factors in flower development. *Genome Biology*

883 **15: R41**

884 **Rajagopalan R, Vaucheret H, Trejo J, Bartel DP** (2006) A diverse and evolutionarily fluid set
885 of microRNAs in *Arabidopsis thaliana*. *Genes Dev* **20**: 3407-3425

886 **Reimer JJ, Turck F** (2010) Genome-wide mapping of protein-DNA interaction by chromatin
887 immunoprecipitation and DNA microarray hybridization (ChIP-chip). Part A: ChIP-chip
888 molecular methods. *Methods Mol Biol* **631**: 139-160

889 **Richter R, Kinoshita A, Vincent C, Martinez-Gallegos R, Gao H, van Driel AD, Hyun Y,**
890 **Mateos JL, Coupland G** (2019) Floral regulators FLC and SOC1 directly regulate
891 expression of the B3-type transcription factor TARGET OF FLC AND SVP 1 at the
892 *Arabidopsis* shoot apex via antagonistic chromatin modifications. *PLoS Genet* **15**:
893 e1008065

894 **Searle I, He Y, Turck F, Vincent C, Fornara F, Krober S, Amasino RA, Coupland G** (2006)
895 The transcription factor FLC confers a flowering response to vernalization by repressing
896 meristem competence and systemic signaling in *Arabidopsis*. *Genes Dev* **20**: 898-912

897 **Szaker HM, Darko E, Medzihradzsky A, Janda T, Liu H-C, Charng Y-Y, Csorba T** (2019)
898 miR824/AGAMOUS-LIKE16 Module Integrates Recurring Environmental Heat Stress
899 Changes to Fine-Tune Poststress Development. *Frontiers in plant science* **10**: 1454

900 **Tao Z, Shen LS, Liu C, Liu L, Yan YY, Yu H** (2012) Genome-wide identification of SOC1 and
901 SVP targets during the floral transition in *Arabidopsis*. *Plant Journal* **70**: 549-561

902 **Thorvaldsdottir H, Robinson JT, Mesirov JP** (2013) Integrative Genomics Viewer (IGV):
903 high-performance genomics data visualization and exploration. *Briefings in Bioinformatics*
904 **14**: 178-192

905 **Tian T, Liu Y, Yan HY, You Q, Yi X, Du Z, Xu WY, Su Z** (2017) agriGO v2.0: a GO analysis
906 toolkit for the agricultural community, 2017 update. *Nucleic Acids Research* **45**:
907 W122-W129

908 **Torti S, Fornara F, Vincent C, Andrés F, Nordström K, Göbel U, Knoll D, Schoof H,**
909 **Coupland G** (2012) Analysis of the *Arabidopsis* Shoot Meristem Transcriptome during
910 Floral Transition Identifies Distinct Regulatory Patterns and a Leucine-Rich Repeat Protein
911 That Promotes Flowering. *Plant Cell* **24**: 444-462

912 **Wang H, Li Y, Pan J, Lou D, Hu Y, Yu D** (2017) The bHLH Transcription Factors MYC2,
913 MYC3, and MYC4 Are Required for Jasmonate-Mediated Inhibition of Flowering in
914 *Arabidopsis*. *Molecular Plant* **10**: 1461-1464

915 **Xiao CW, Chen FL, Yu XH, Lin CT, Fu YF** (2009) Over-expression of an AT-hook gene,

916 AHL22, delays flowering and inhibits the elongation of the hypocotyl in *Arabidopsis thaliana*.
917 *Plant Molecular Biology* **71**: 39-50

918 **Yan F-H, Zhang L-P, Cheng F, Yu D-M, Hu J-Y** (2021) Accession-specific flowering time
919 variation in response to nitrate fluctuation in *Arabidopsis thaliana*. *Plant Diversity* **43**: 78-85

920 **Yoo SD, Cho YH, Sheen J** (2007) *Arabidopsis* mesophyll protoplasts: a versatile cell system
921 for transient gene expression analysis. *Nature Protocols* **2**: 1565-1572

922 **Yu D, Dong X, Zou K, Jiang X-D, Sun Y-B, Min Z, Zhang L-P, Cui H, Hu J-Y** (2022) A hidden
923 mutation in the seventh WD40-repeat of COP1 determines the early flowering trait in a set
924 of *Arabidopsis* myc mutants. *The Plant Cell*

925 **Yu GC, Wang LG, He QY** (2015) ChIPseeker: an R/Bioconductor package for ChIP peak
926 annotation, comparison and visualization. *Bioinformatics* **31**: 2382-2383

927 **Zhai Q, Zhang X, Wu F, Feng H, Deng L, Xu L, Zhang M, Wang Q, Li C** (2015)
928 Transcriptional Mechanism of Jasmonate Receptor CO11-Mediated Delay of Flowering
929 Time in *Arabidopsis*. *The Plant Cell* **27**: 2814-2828

930 **Zhang Y, Liu T, Meyer CA, Eeckhoutte J, Johnson DS, Bernstein BE, Nussbaum C, Myers**
931 **RM, Brown M, Li W, Liu XS** (2008) Model-based Analysis of ChIP-Seq (MACS). *Genome*
932 *Biology* **9**: 9

933 **Zhao C, Hanada A, Yamaguchi S, Kamiya Y, Beers EP** (2011) The *Arabidopsis* Myb genes
934 MYR1 and MYR2 are redundant negative regulators of flowering time under decreased
935 light intensity. *Plant J* **66**: 502-515

936 **Zhao P-X, Miao Z-Q, Zhang J, Chen S-Y, Liu Q-Q, Xiang C-B** (2020) MADS-box factor
937 AGL16 negatively regulates drought resistance via stomatal density and stomatal
938 movement. *Journal of experimental botany* **71**: 6092-6610

939 **Zhao PX, Zhang J, Chen SY, Wu J, Xia JQ, Sun LQ, Ma SS, Xiang CB** (2021) *Arabidopsis*
940 MADS-box factor AGL16 is a negative regulator of plant response to salt stress by
941 downregulating salt-responsive genes. *New Phytologist* **232**: 2418-2439

942 **Zhou Y, Hartwig B, James GV, Schneeberger K, Turck F** (2016) Complementary Activities
943 of TELOMERE REPEAT BINDING Proteins and Polycomb Group Complexes in
944 Transcriptional Regulation of Target Genes. *The Plant Cell* **28**: 87-101

945

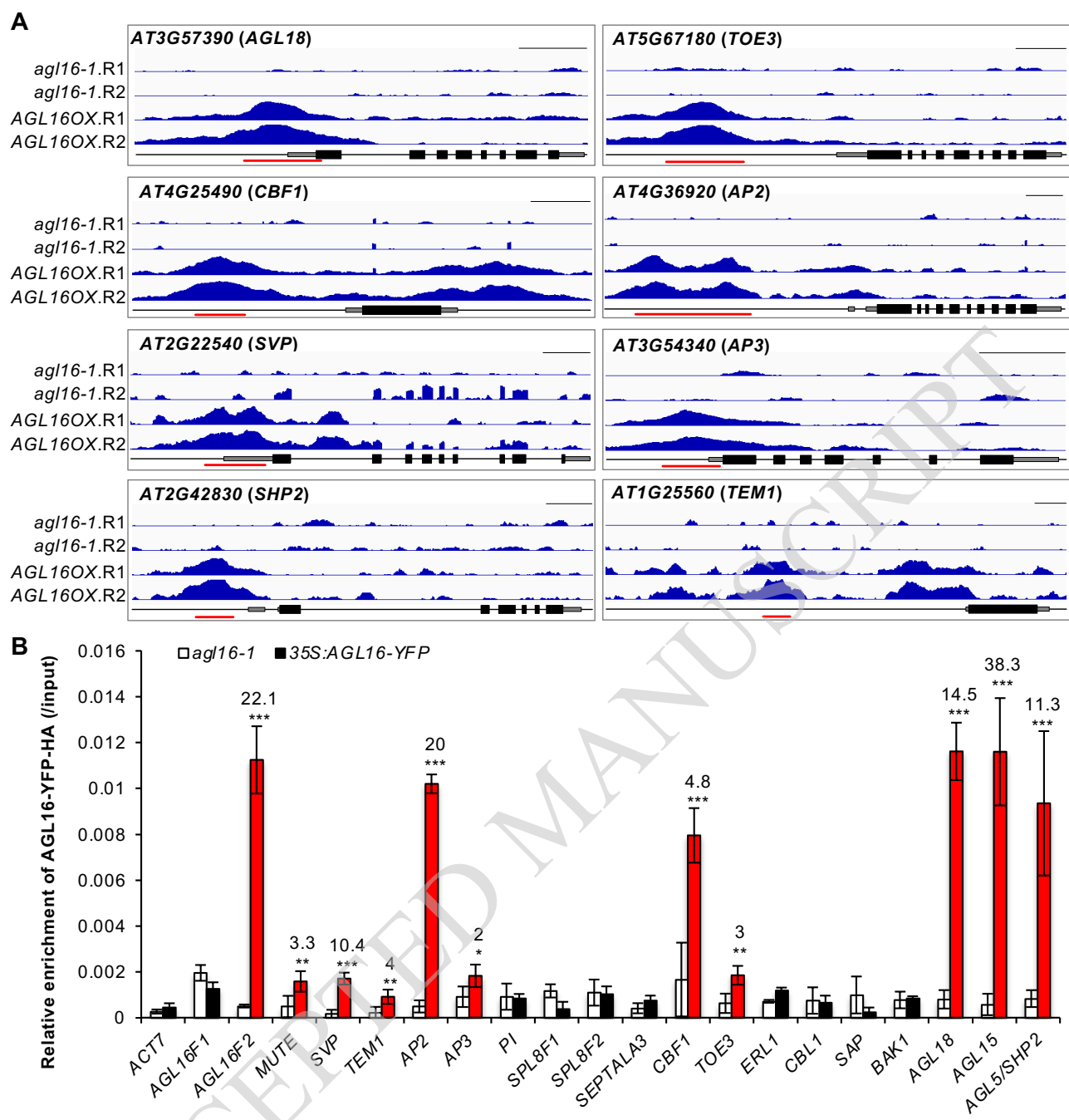


Fig. 1 Validation of the AGL16 binding on target DNA fragments.

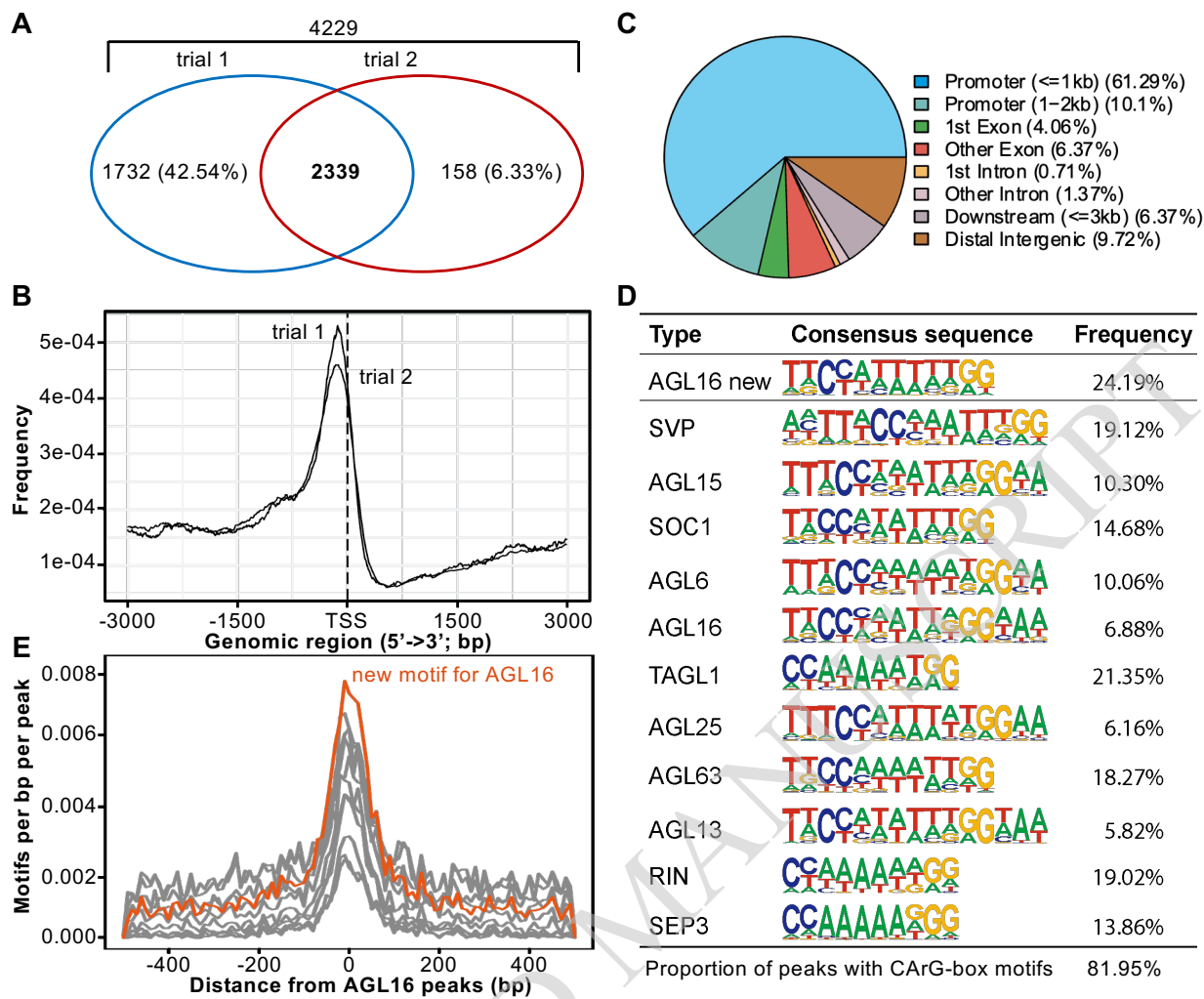


Fig. 2 Genome-wide identification of AGL16 target genes via ChIP-seq.

ACCEPTED

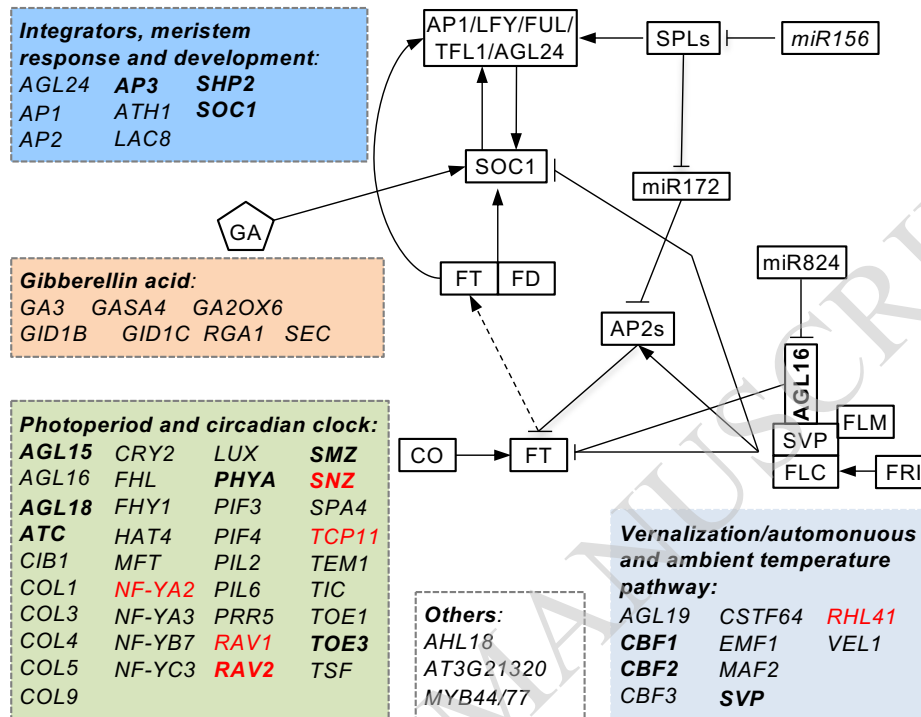


Fig. 3 Molecular pathways (indicated with different color boxes) targeted by AGL16.

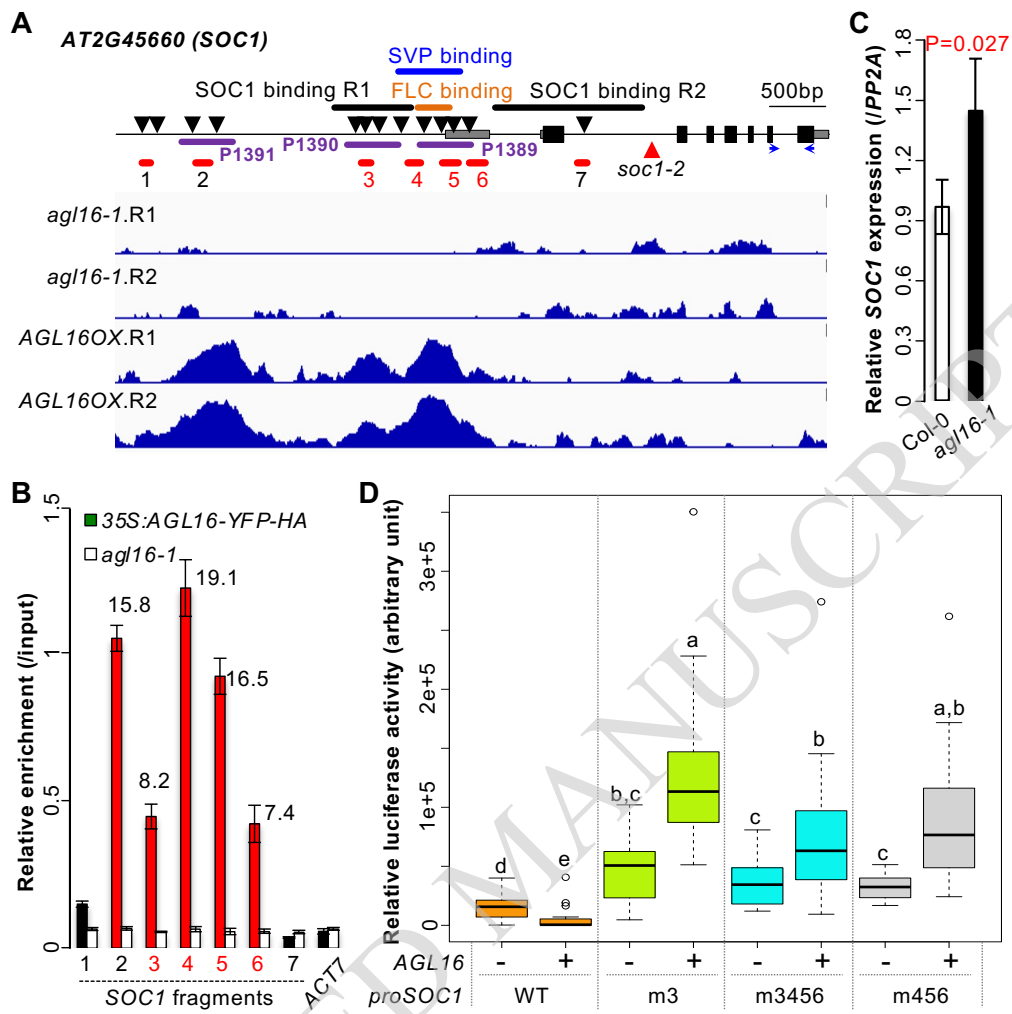


Fig. 4 AGL16 targets *SOC1* and represses its expression.

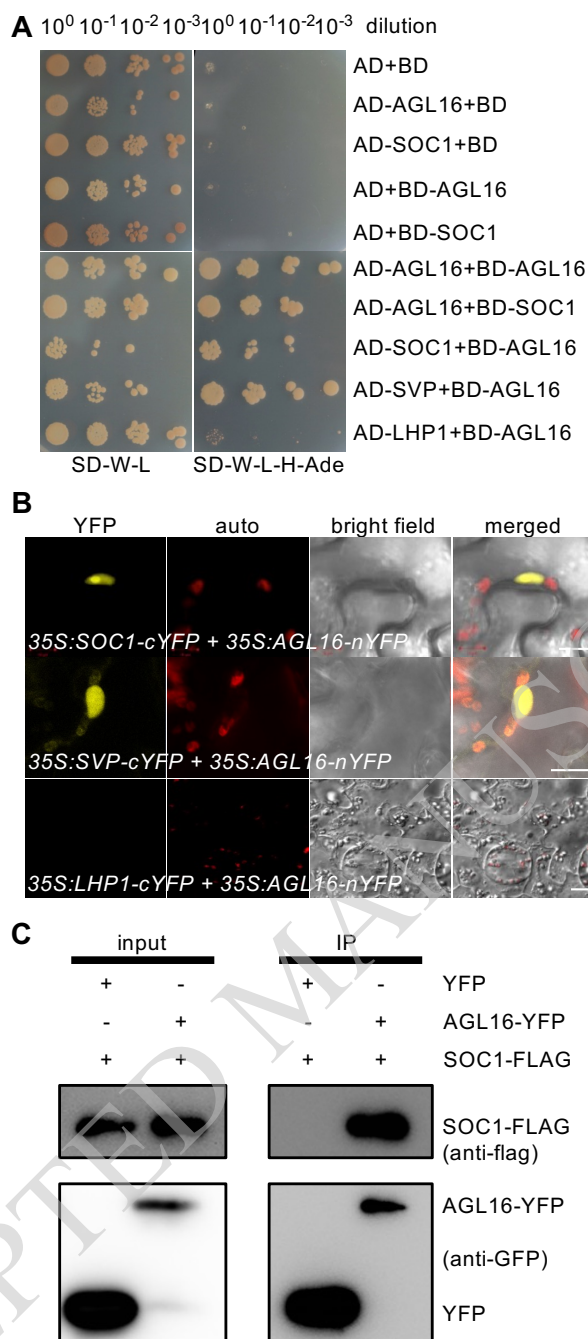


Fig. 5 AGL16 forms protein complex with SOC1.

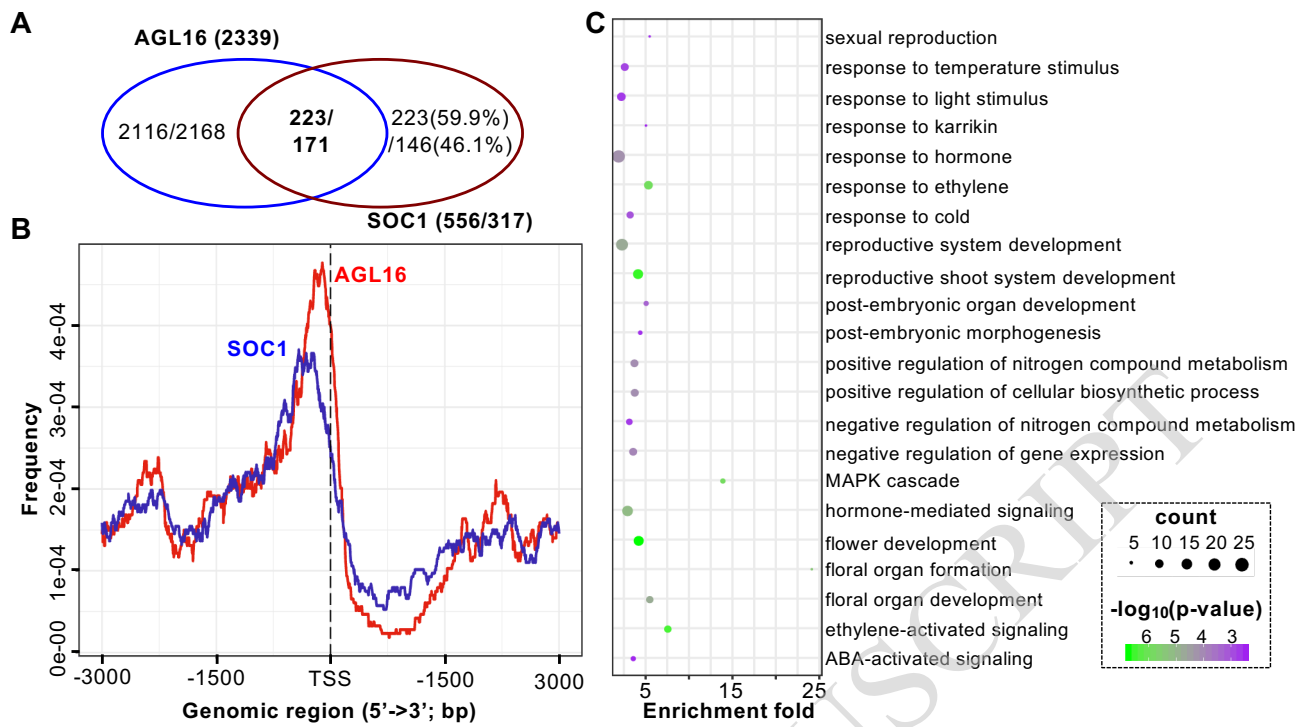


Fig. 6 AGL16 and SOC1 share a common set of target genes involved in multiple functions.

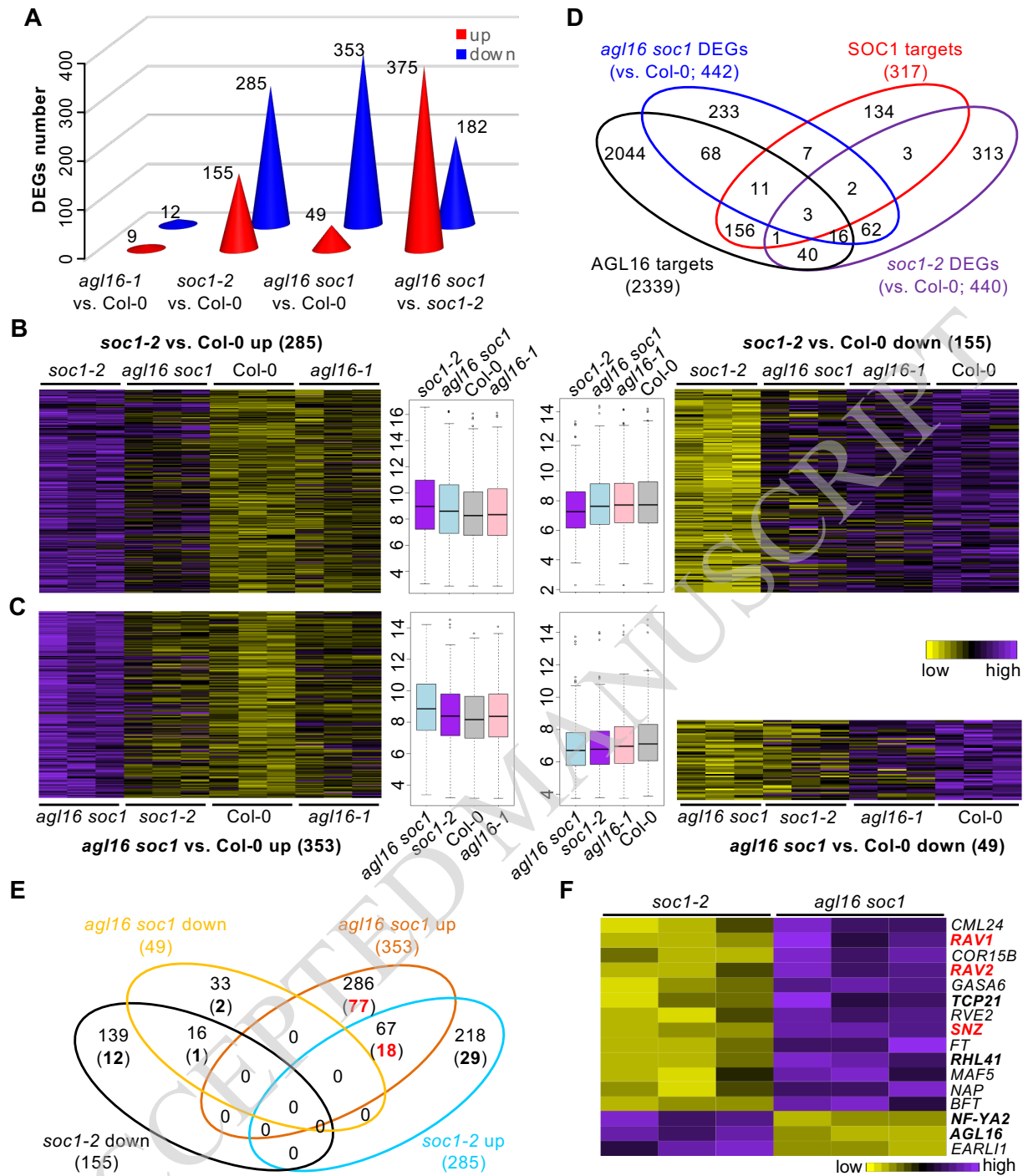


Fig. 7 The *AGL16-SOC1* module collaborates on regulation of genome-wide gene expression.



Fig. 8 AGL16 and SOC1 regulate additively flowering time.

ACCEPTED MANUSCRIPT

Parsed Citations

- Aerts N, de Bruijn S, van Mourik H, Angenent GC, van Dijk ADJ (2018) Comparative analysis of binding patterns of MADS-domain proteins in *Arabidopsis thaliana*. *BMC Plant Biology* 18: 131
Google Scholar: [Author Only](#) [Title Only](#) [Author and Title](#)
- Alvarez-Buylla ER, Liljegren SJ, Pelaz S, Gold SE, Burgeff C, Ditta GS, Vergara-Silva F, Yanofsky MF (2000) MADS-box gene evolution beyond flowers: expression in pollen, endosperm, guard cells, roots and trichomes. *Plant J* 24: 457-466
Google Scholar: [Author Only](#) [Title Only](#) [Author and Title](#)
- Andres F, Coupland G (2012) The genetic basis of flowering responses to seasonal cues. *Nat Rev Genet* 13: 627-639
Google Scholar: [Author Only](#) [Title Only](#) [Author and Title](#)
- Aukerman MJ, Sakai H (2003) Regulation of flowering time and floral organ identity by a MicroRNA and its APETALA2-like target genes. *Plant Cell* 15: 2730-2741
Google Scholar: [Author Only](#) [Title Only](#) [Author and Title](#)
- Bao S, Hua C, Huang G, Cheng P, Gong X, Shen L, Yu H (2019) Molecular Basis of Natural Variation in Photoperiodic Flowering Responses. *Developmental Cell* 50: 90-101.e103
Google Scholar: [Author Only](#) [Title Only](#) [Author and Title](#)
- Bouche F, Lobet G, Tocquin P, Perilleux C (2016) FLOR-ID: an interactive database of flowering-time gene networks in *Arabidopsis thaliana*. *Nucleic Acids Research* 44: D1167-D1171
Google Scholar: [Author Only](#) [Title Only](#) [Author and Title](#)
- Boxall SF, Foster JM, Bohnert HJ, Cushman JC, Nimmo HG, Hartwell J (2005) Conservation and Divergence of Circadian Clock Operation in a Stress-Inducible Crassulacean Acid Metabolism Species Reveals Clock Compensation against Stress. *Plant Physiology* 137: 969-982
Google Scholar: [Author Only](#) [Title Only](#) [Author and Title](#)
- Castillejo C, Pelaz S (2008) The balance between CONSTANS and TEMPRANILLO activities determines FT expression to trigger flowering. *Curr Biol* 18: 1338-1343
Google Scholar: [Author Only](#) [Title Only](#) [Author and Title](#)
- Chen Y, Zhang L, Zhang H, Chen L, Yu D (2021) ERF1 delays flowering through direct inhibition of FLOWERING LOCUS T expression in *Arabidopsis*. *J Integr Plant Biol* 63: 1712-1723
Google Scholar: [Author Only](#) [Title Only](#) [Author and Title](#)
- Corbesier L, Vincent C, Jang S, Fornara F, Fan Q, Searle I, Giakountis A, Farrona S, Gissot L, Turnbull C, Coupland G (2007) FT protein movement contributes to long-distance signaling in floral induction of *Arabidopsis*. *Science* 316: 1030-1033
Google Scholar: [Author Only](#) [Title Only](#) [Author and Title](#)
- Crevillen P, Sonmez C, Wu Z, Dean C (2013) A gene loop containing the floral repressor FLC is disrupted in the early phase of vernalization. *EMBO J* 32: 140-148
Google Scholar: [Author Only](#) [Title Only](#) [Author and Title](#)
- Cui HT, Qiu JD, Zhou Y, Bhandari DD, Zhao CH, Bautor J, Parker JE (2018) Antagonism of Transcription Factor MYC2 by EDS1/PAD4 Complexes Bolsters Salicylic Acid Defense in *Arabidopsis* Effector-Triggered Immunity. *Molecular Plant* 11: 1053-1066
Google Scholar: [Author Only](#) [Title Only](#) [Author and Title](#)
- Das SS, Yadav S, Singh A, Gautam V, Sarkar AK, Nandi AK, Karmakar P, Majee M, Sanan-Mishra N (2018) Expression dynamics of miRNAs and their targets in seed germination conditions reveals miRNA-ta-siRNA crosstalk as regulator of seed germination. *Scientific Reports* 8: 13
Google Scholar: [Author Only](#) [Title Only](#) [Author and Title](#)
- de Folter S, Immink RG, Kieffer M, Parenicova L, Henz SR, Weigel D, Busscher M, Kooiker M, Colombo L, Kater MM, Davies B, Angenent GC (2005) Comprehensive interaction map of the *Arabidopsis* MADS Box transcription factors. *Plant Cell* 17: 1424-1433
Google Scholar: [Author Only](#) [Title Only](#) [Author and Title](#)
- de Meaux J, Hu JY, Tartler U, Goebel U (2008) Structurally different alleles of the ath-MIR824 microRNA precursor are maintained at high frequency in *Arabidopsis thaliana*. *Proc Natl Acad Sci U S A* 105: 8994-8999
Google Scholar: [Author Only](#) [Title Only](#) [Author and Title](#)
- Deng W, Ying H, Helliwell CA, Taylor JM, Peacock WJ, Dennis ES (2011) FLOWERING LOCUS C (FLC) regulates development pathways throughout the life cycle of *Arabidopsis*. *Proc Natl Acad Sci U S A* 108: 6680-6685
Google Scholar: [Author Only](#) [Title Only](#) [Author and Title](#)
- Fahlgren N, Howell MD, Kasschau KD, Chapman EJ, Sullivan CM, Cumbie JS, Givan SA, Law TF, Grant SR, Dangl JL, Carrington JC (2007) High-throughput sequencing of *Arabidopsis* microRNAs: evidence for frequent birth and death of MIRNA genes. *PLoS One* 2: e219

Google Scholar: [Author Only](#) [Title Only](#) [Author and Title](#)

Fornara F, de Montaigu A, Coupland G (2010) Snapshot: Control of flowering in Arabidopsis. Cell 141: 550, 550 e551-552

Google Scholar: [Author Only](#) [Title Only](#) [Author and Title](#)

Gregis V, Andres F, Sessa A, Guerra R, Simonini S, Mateos J, Torti S, Zambelli F, Prazzoli G, Bjerkan K, Grini P, Pavasi G, Colombo L, Coupland G, Kater M (2013) Identification of pathways directly regulated by SHORT VEGETATIVE PHASE during vegetative and reproductive development in Arabidopsis. Genom Biol 14: R56

Google Scholar: [Author Only](#) [Title Only](#) [Author and Title](#)

Heinz S, Benner C, Spann N, Bertolino E, Lin YC, Laslo P, Cheng JX, Murre C, Singh H, Glass CK (2010) Simple Combinations of Lineage-Determining Transcription Factors Prime cis-Regulatory Elements Required for Macrophage and B Cell Identities. Molecular Cell 38: 576-589

Google Scholar: [Author Only](#) [Title Only](#) [Author and Title](#)

Hepworth SR, Valverde F, Ravenscroft D, Mouradov A, Coupland G (2002) Antagonistic regulation of flowering-time gene SOC1 by CONSTANS and FLC via separate promoter motifs. EMBO J 21: 4327-4337

Google Scholar: [Author Only](#) [Title Only](#) [Author and Title](#)

Hu JY, Zhou Y, He F, Dong X, Liu LY, Coupland G, Turck F, de Meaux J (2014) miR824-Regulated AGAMOUS-LIKE16 Contributes to Flowering Time Repression in Arabidopsis. Plant Cell 26: 2024-2037

Google Scholar: [Author Only](#) [Title Only](#) [Author and Title](#)

Hwang K, Susila H, Nasim Z, Jung J-Y, Ahn JH (2019) Arabidopsis ABF3 and ABF4 Transcription Factors Act with the NF-YC Complex to Regulate SOC1 Expression and Mediate Drought-Accelerated Flowering. Molecular Plant 12: 489-505

Google Scholar: [Author Only](#) [Title Only](#) [Author and Title](#)

Hyun Y, Richter R, Vincent C, Martinez-Gallegos R, Porri A, Coupland G (2016) Multi-layered Regulation of SPL15 and Cooperation with SOC1 Integrate Endogenous Flowering Pathways at the Arabidopsis Shoot Meristem. Developmental Cell 37: 254-266

Google Scholar: [Author Only](#) [Title Only](#) [Author and Title](#)

Immink RG, Tonaco IA, de Folter S, Shchennikova A, van Dijk AD, Busscher-Lange J, Borst JW, Angenent GC (2009) SEPALLATA3: the 'glue' for MADS box transcription factor complex formation. Genome Biol 10: R24

Google Scholar: [Author Only](#) [Title Only](#) [Author and Title](#)

Immink RGH, Posé D, Ferrario S, Ott F, Kaufmann K, Valentim FL, de Folter S, van der Wal F, van Dijk ADJ, Schmid M, Angenent GC (2012) Characterization of SOC1's Central Role in Flowering by the Identification of Its Upstream and Downstream Regulators. Plant Physiology 160: 433-449

Google Scholar: [Author Only](#) [Title Only](#) [Author and Title](#)

Johanson U, West J, Lister C, Michaels S, Amasino R, Dean C (2000) Molecular Analysis of FRIGIDA, a Major Determinant of Natural Variation in Arabidopsis Flowering Time. Science 290: 344-347

Google Scholar: [Author Only](#) [Title Only](#) [Author and Title](#)

Jung JH, Ju Y, Seo PJ, Lee JH, Park CM (2012) The SOC1-SPL module integrates photoperiod and gibberellic acid signals to control flowering time in Arabidopsis. Plant J 69: 577-588

Google Scholar: [Author Only](#) [Title Only](#) [Author and Title](#)

Jung JH, Seo YH, Seo PJ, Reyes JL, Yun J, Chua NH, Park CM (2007) The GIGANTEA-regulated microRNA172 mediates photoperiodic flowering independent of CONSTANS in Arabidopsis. Plant Cell 19: 2736-2748

Google Scholar: [Author Only](#) [Title Only](#) [Author and Title](#)

Kaufmann K, Muino JM, Jauregui R, Airoidi CA, Smaczniak C, Krajewski P, Angenent GC (2009) Target genes of the MADS transcription factor SEPALLATA3: integration of developmental and hormonal pathways in the Arabidopsis flower. PLoS Biol 7: e1000090

Google Scholar: [Author Only](#) [Title Only](#) [Author and Title](#)

Kaufmann K, Wellmer F, Muino JM, Ferrier T, Wuest SE, Kumar V, Serrano-Mislata A, Madueno F, Krajewski P, Meyerowitz EM, Angenent GC, Riechmann JL (2010) Orchestration of floral initiation by APETALA1. Science 328: 85-89

Google Scholar: [Author Only](#) [Title Only](#) [Author and Title](#)

Kazan K, Manners JM (2013) MYC2: The Master in Action. Molecular Plant 6: 686-703

Google Scholar: [Author Only](#) [Title Only](#) [Author and Title](#)

Kim D, Paggi JM, Park C, Bennett C, Salzberg SL (2019) Graph-based genome alignment and genotyping with HISAT2 and HISAT-genotype. Nature Biotechnology 37: 907-+

Google Scholar: [Author Only](#) [Title Only](#) [Author and Title](#)

Kutter C, Schob H, Stadler M, Meins F, Jr., Si-Ammour A (2007) MicroRNA-mediated regulation of stomatal development in Arabidopsis. Plant Cell 19: 2417-2429

Google Scholar: [Author Only](#) [Title Only](#) [Author and Title](#)

Lee J, Lee I (2010) Regulation and function of SOC1, a flowering pathway integrator. *Journal of Experimental Botany* 61: 2247-2254

Google Scholar: [Author Only](#) [Title Only](#) [Author and Title](#)

Lee J, Oh M, Park H, Lee I (2008) SOC1 translocated to the nucleus by interaction with AGL24 directly regulates leafy. *Plant J* 55: 832-843

Google Scholar: [Author Only](#) [Title Only](#) [Author and Title](#)

Li D, Liu C, Shen L, Wu Y, Chen H, Robertson M, Helliwell CA, Ito T, Meyerowitz E, Yu H (2008) A repressor complex governs the integration of flowering signals in *Arabidopsis*. *Dev Cell* 15: 110-120

Google Scholar: [Author Only](#) [Title Only](#) [Author and Title](#)

Li H (2013) Aligning sequence reads, clone sequences and assembly contigs with BWA-MEM. arXiv: 1303.3997

Google Scholar: [Author Only](#) [Title Only](#) [Author and Title](#)

Li H, Handsaker B, Wysoker A, Fennell T, Ruan J, Homer N, Marth G, Abecasis G, Durbin R, Genome Project Data P (2009) The Sequence Alignment/Map format and SAMtools. *Bioinformatics* 25: 2078-2079

Google Scholar: [Author Only](#) [Title Only](#) [Author and Title](#)

Li H, Ye K, Shi Y, Cheng J, Zhang X, Yang S (2017) BZR1 Positively Regulates Freezing Tolerance via CBF-Dependent and CBF-Independent Pathways in *Arabidopsis*. *Molecular Plant* 10: 545-559

Google Scholar: [Author Only](#) [Title Only](#) [Author and Title](#)

Liao Y, Smyth GK, Shi W (2013) The Subread aligner: fast, accurate and scalable read mapping by seed-and-vote. *Nucleic Acids Research* 41

Google Scholar: [Author Only](#) [Title Only](#) [Author and Title](#)

Liao Y, Smyth GK, Shi W (2014) featureCounts: an efficient general purpose program for assigning sequence reads to genomic features. *Bioinformatics* 30: 923-930

Google Scholar: [Author Only](#) [Title Only](#) [Author and Title](#)

Liu L, Adrian J, Pankin A, Hu J, Dong X, von Korff M, Turck F (2014) Induced and natural variation of promoter length modulates the photoperiodic response of FLOWERING LOCUS T. *Nat Commun* 5

Google Scholar: [Author Only](#) [Title Only](#) [Author and Title](#)

Liu T, Li Y, Ren J, Qian Y, Yang X, Duan W, Hou X (2013) Nitrate or NaCl regulates floral induction in *Arabidopsis thaliana*. *Biologia* 68: 215-222

Google Scholar: [Author Only](#) [Title Only](#) [Author and Title](#)

Machanic P, Bailey TL (2011) MEME-ChIP: motif analysis of large DNA datasets. *Bioinformatics* 27: 1696-1697

Google Scholar: [Author Only](#) [Title Only](#) [Author and Title](#)

Mateos J, Madrigal P, Tsuda K, Rawat V, Richter R, Romera-Branchat M, Fornara F, Schneeberger K, Krajewski P, Coupland G (2015) Combinatorial activities of SHORT VEGETATIVE PHASE and FLOWERING LOCUS C define distinct modes of flowering regulation in *Arabidopsis*. *Genome Biology* 16: 31

Google Scholar: [Author Only](#) [Title Only](#) [Author and Title](#)

Mateos JL, Tilmes V, Madrigal P, Severing E, Richter R, Rijkenberg CWM, Krajewski P, Coupland G (2017) Divergence of regulatory networks governed by the orthologous transcription factors FLC and PEP1 in Brassicaceae species. *Proc Natl Acad Sci U S A* 114: E11037-E11046

Google Scholar: [Author Only](#) [Title Only](#) [Author and Title](#)

Mathieu J, Yant LJ, Murdter F, Kuttner F, Schmid M (2009) Repression of flowering by the miR172 target SMZ. *PLoS Biol* 7: e1000148

Google Scholar: [Author Only](#) [Title Only](#) [Author and Title](#)

Mi HY, Huang XS, Muruganujan A, Tang HM, Mills C, Kang D, Thomas PD (2017) PANTHER version 11: expanded annotation data from Gene Ontology and Reactome pathways, and data analysis tool enhancements. *Nucleic Acids Research* 45: D183-D189

Google Scholar: [Author Only](#) [Title Only](#) [Author and Title](#)

Michaels SD (2009) Flowering time regulation produces much fruit. *Curr Opin Plant Biol* 12: 75-80

Google Scholar: [Author Only](#) [Title Only](#) [Author and Title](#)

Michaels SD, Amasino RM (2001) Loss of FLOWERING LOCUS C activity eliminates the late-flowering phenotype of FRIGIDA and autonomous pathway mutations but not responsiveness to vernalization. *Plant Cell* 13: 935-941

Google Scholar: [Author Only](#) [Title Only](#) [Author and Title](#)

Nee G, Xiang Y, Soppe WJJ (2017) The release of dormancy, a wake-up call for seeds to germinate. *Current Opinion in Plant Biology* 35: 8-14

Google Scholar: [Author Only](#) [Title Only](#) [Author and Title](#)

Olas JJ, Van Dingenen J, Abel C, Dzialo MA, Feil R, Krapp A, Schlereth A, Wahl V (2019) Nitrate acts at the Arabidopsis thaliana shoot apical meristem to regulate flowering time. *The New phytologist* 223: 814-827

Google Scholar: [Author Only](#) [Title Only](#) [Author and Title](#)

Pajoro A, Madrigal P, Muiño JM, Matus JT, Jin J, Mecchia MA, Debernardi JM, Palatnik JF, Balazadeh S, Arif M, Ó'Maoiléidigh DS, Wellmer F, Krajewski P, Riechmann J-L, Angenent GC, Kaufmann K (2014) Dynamics of chromatin accessibility and gene regulation by MADS-domain transcription factors in flower development. *Genome Biology* 15: R41

Google Scholar: [Author Only](#) [Title Only](#) [Author and Title](#)

Rajagopalan R, Vaucheret H, Trejo J, Bartel DP (2006) A diverse and evolutionarily fluid set of microRNAs in Arabidopsis thaliana. *Genes Dev* 20: 3407-3425

Google Scholar: [Author Only](#) [Title Only](#) [Author and Title](#)

Reimer JJ, Turck F (2010) Genome-wide mapping of protein-DNA interaction by chromatin immunoprecipitation and DNA microarray hybridization (ChIP-chip). Part A: ChIP-chip molecular methods. *Methods Mol Biol* 631: 139-160

Google Scholar: [Author Only](#) [Title Only](#) [Author and Title](#)

Richter R, Kinoshita A, Vincent C, Martinez-Gallegos R, Gao H, van Driel AD, Hyun Y, Mateos JL, Coupland G (2019) Floral regulators FLC and SOC1 directly regulate expression of the B3-type transcription factor TARGET OF FLC AND SVP 1 at the Arabidopsis shoot apex via antagonistic chromatin modifications. *PLoS Genet* 15: e1008065

Google Scholar: [Author Only](#) [Title Only](#) [Author and Title](#)

Searle I, He Y, Turck F, Vincent C, Fornara F, Krober S, Amasino RA, Coupland G (2006) The transcription factor FLC confers a flowering response to vernalization by repressing meristem competence and systemic signaling in Arabidopsis. *Genes Dev* 20: 898-912

Google Scholar: [Author Only](#) [Title Only](#) [Author and Title](#)

Szaker HM, Darko E, Medzihradzky A, Janda T, Liu H-C, Charng Y-Y, Csorba T (2019) miR824/AGAMOUS-LIKE16 Module Integrates Recurring Environmental Heat Stress Changes to Fine-Tune Poststress Development. *Frontiers in plant science* 10: 1454

Google Scholar: [Author Only](#) [Title Only](#) [Author and Title](#)

Tao Z, Shen LS, Liu C, Liu L, Yan YY, Yu H (2012) Genome-wide identification of SOC1 and SVP targets during the floral transition in Arabidopsis. *Plant Journal* 70: 549-561

Google Scholar: [Author Only](#) [Title Only](#) [Author and Title](#)

Thorvaldsdottir H, Robinson JT, Mesirov JP (2013) Integrative Genomics Viewer (IGV): high-performance genomics data visualization and exploration. *Briefings in Bioinformatics* 14: 178-192

Google Scholar: [Author Only](#) [Title Only](#) [Author and Title](#)

Tian T, Liu Y, Yan HY, You Q, Yi X, Du Z, Xu WY, Su Z (2017) agriGO v2.0: a GO analysis toolkit for the agricultural community, 2017 update. *Nucleic Acids Research* 45: W122-W129

Google Scholar: [Author Only](#) [Title Only](#) [Author and Title](#)

Torti S, Fornara F, Vincent C, Andrés F, Nordström K, Göbel U, Knoll D, Schoof H, Coupland G (2012) Analysis of the Arabidopsis Shoot Meristem Transcriptome during Floral Transition Identifies Distinct Regulatory Patterns and a Leucine-Rich Repeat Protein That Promotes Flowering. *Plant Cell* 24: 444-462

Google Scholar: [Author Only](#) [Title Only](#) [Author and Title](#)

Wang H, Li Y, Pan J, Lou D, Hu Y, Yu D (2017) The bHLH Transcription Factors MYC2, MYC3, and MYC4 Are Required for Jasmonate-Mediated Inhibition of Flowering in Arabidopsis. *Molecular Plant* 10: 1461-1464

Google Scholar: [Author Only](#) [Title Only](#) [Author and Title](#)

Xiao CW, Chen FL, Yu XH, Lin CT, Fu YF (2009) Over-expression of an AT-hook gene, AHL22, delays flowering and inhibits the elongation of the hypocotyl in Arabidopsis thaliana. *Plant Molecular Biology* 71: 39-50

Google Scholar: [Author Only](#) [Title Only](#) [Author and Title](#)

Yan F-H, Zhang L-P, Cheng F, Yu D-M, Hu J-Y (2021) Accession-specific flowering time variation in response to nitrate fluctuation in Arabidopsis thaliana. *Plant Diversity* 43: 78-85

Google Scholar: [Author Only](#) [Title Only](#) [Author and Title](#)

Yoo SD, Cho YH, Sheen J (2007) Arabidopsis mesophyll protoplasts: a versatile cell system for transient gene expression analysis. *Nature Protocols* 2: 1565-1572

Google Scholar: [Author Only](#) [Title Only](#) [Author and Title](#)

Yu D, Dong X, Zou K, Jiang X-D, Sun Y-B, Min Z, Zhang L-P, Cui H, Hu J-Y (2022) A hidden mutation in the seventh WD40-repeat of COP1 determines the early flowering trait in a set of Arabidopsis myc mutants. *The Plant Cell*

Google Scholar: [Author Only](#) [Title Only](#) [Author and Title](#)

Yu GC, Wang LG, He QY (2015) ChIPseeker: an R/Bioconductor package for ChIP peak annotation, comparison and visualization. *Bioinformatics* 31: 2382-2383

Google Scholar: [Author Only](#) [Title Only](#) [Author and Title](#)

Zhai Q, Zhang X, Wu F, Feng H, Deng L, Xu L, Zhang M, Wang Q, Li C (2015) Transcriptional Mechanism of Jasmonate Receptor COI1-Mediated Delay of Flowering Time in Arabidopsis. *The Plant Cell* 27: 2814-2828

Google Scholar: [Author Only](#) [Title Only](#) [Author and Title](#)

Zhang Y, Liu T, Meyer CA, Eeckhoutte J, Johnson DS, Bernstein BE, Nussbaum C, Myers RM, Brown M, Li W, Liu XS (2008) Model-based Analysis of ChIP-Seq (MACS). *Genome Biology* 9: 9

Google Scholar: [Author Only](#) [Title Only](#) [Author and Title](#)

Zhao C, Hanada A, Yamaguchi S, Kamiya Y, Beers EP (2011) The Arabidopsis Myb genes MYR1 and MYR2 are redundant negative regulators of flowering time under decreased light intensity. *Plant J* 66: 502-515

Google Scholar: [Author Only](#) [Title Only](#) [Author and Title](#)

Zhao P-X, Miao Z-Q, Zhang J, Chen S-Y, Liu Q-Q, Xiang C-B (2020) MADS-box factor AGL16 negatively regulates drought resistance via stomatal density and stomatal movement. *Journal of experimental botany* 71: 6092-6610

Google Scholar: [Author Only](#) [Title Only](#) [Author and Title](#)

Zhao PX, Zhang J, Chen SY, Wu J, Xia JQ, Sun LQ, Ma SS, Xiang CB (2021) Arabidopsis MADS-box factor AGL16 is a negative regulator of plant response to salt stress by downregulating salt-responsive genes. *New Phytologist* 232: 2418-2439

Google Scholar: [Author Only](#) [Title Only](#) [Author and Title](#)

Zhou Y, Hartwig B, James GV, Schneeberger K, Turck F (2016) Complementary Activities of TELOMERE REPEAT BINDING Proteins and Polycomb Group Complexes in Transcriptional Regulation of Target Genes. *The Plant Cell* 28: 87-101

Google Scholar: [Author Only](#) [Title Only](#) [Author and Title](#)

ACCEPTED MANUSCRIPT